AD-A120 169 NAVAL RESEARCH LAB WASHINGTON DC F/G 13/1h
MEASUREMENTS OF OPTICAL TURBULENCE PARAMETERS ABOARD THE AIRCRA--ETC(U)
SEP 82 D R CUTTEN
UNCLASSIFIED NRL-MR-4911 NL

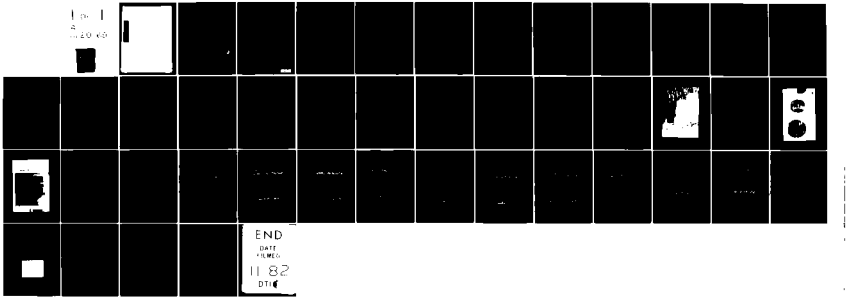

SECURITY CLASSIFICATION OF THIS PAGE (When Data Entered)

REPORT DOCUMENTATION PAGE		READ INSTRUCTIONS BEFORE COMPLETING FORM
1. REPORT NUMBER NRL Memorandum Report 4911	2. GOVT ACCESSION NO. AD-A120169	3. RECIPIENT'S CATALOG NUMBER
4. TITLE (and Subtitle) MEASUREMENTS OF OPTICAL TURBULENCE PARAMETERS ABOARD THE AIRCRAFT CARRIER USS LEXINGTON		5. TYPE OF REPORT & PERIOD COVERED Interim report on a continuing NRL problem. 6. PERFORMING ORG. REPORT NUMBER
7. AUTHOR(s) D.R. Cutten*		8. CONTRACT OR GRANT NUMBER(s)
9. PERFORMING ORGANIZATION NAME AND ADDRESS Naval Research Laboratory Washington, DC 20375		10. PROGRAM ELEMENT, PROJECT, TASK AREA & WORK UNIT NUMBERS 63754N; 62759N; S0182AA; SF59551697; F2020; F202A; 65-F201-0-2
11. CONTROLLING OFFICE NAME AND ADDRESS Naval Sea Systems Command Washington, DC 20362 Naval Ocean Systems Center San Diego, CA 92152		12. REPORT DATE September 30, 1982 13. NUMBER OF PAGES 43
14. MONITORING AGENCY NAME & ADDRESS(if different from Controlling Office)		15. SECURITY CLASS. (of this report) UNCLASSIFIED 15a. DECLASSIFICATION/DOWNGRADING SCHEDULE

16. DISTRIBUTION STATEMENT (of this Report)

Approved for public release; distribution unlimited.

17. DISTRIBUTION STATEMENT (of the abstract entered in Block 20, if different from Report)

18. SUPPLEMENTARY NOTES

*Present address: Electronics Research Laboratory, Salisbury, South Australia

19. KEY WORDS (Continue on reverse side if necessary and identify by block number)

Optical turbulence
C_N^2 (Refractive index structure parameter)

20. ABSTRACT (Continue on reverse side if necessary and identify by block number)

This report presents measurements of optical turbulence at several locations on board the USS LEXINGTON. Data on C_N^2 were collected during and outside flight operations at three sites using a set of microthermal probes. Background values of C_N^2 were found generally to be $10^{-15} m^{-2/3}$ or less while spikes 2 to 3 orders greater are observed during aircraft launch. High values of C_N^2 measured at the hanger bay door are used to estimate a new error for the pointing accuracy of the ship-to-ship tracker due to beam wander. The bulk parameterization model is also used with moderate success to predict background C_N^2. Finally several C_N^2 frequency spectra are presented and their usefulness discussed.

DD FORM 1 JAN 73 1473 EDITION OF 1 NOV 65 IS OBSOLETE
S/N 0102-014-6601

SECURITY CLASSIFICATION OF THIS PAGE (When Data Entered)

C(sq. N)

10^{-15}th power/$m^{(2/3)}$

CONTENTS

MEASUREMENTS OF OPTICAL TURBULENCE PARAMETERS ABOARD THE AIRCRAFT CARRIER USS LEXINGTON

I. INTRODUCTION

The purpose of this paper is to report on further results of optical turbulence measurements made on board the aircraft carrier, USS LEXINGTON, while on training operations in the Gulf of Mexico. These measurements were a follow-up to measurements made on the same ship in July, 1979[1] which had revealed several phenomena requiring further interpretation.

A knowledge of near-ship effects on optical turbulence are required as preparatory to the at-sea, long-path DF laser transmission measurements over water; the USS LEXINGTON is proposed to be used as the transmitter platform for these experiments. Furthermore, this data will extend the Ship's Atmosphere model base.

2. OPTICAL TURBULENCE MEASUREMENTS

The most popular model for predicting small scale fluctuations in the optical index of refraction is based on fluctuations in temperature and humidity. In the inertial subrange of locally isotropic turbulence, the magnitude of the fluctuations can be represented by the structure function parameters for temperature (C_T^2) and humidity (C_q^2). Thus, the refractive index structure parameter (C_N^2) can be written[2]

$$C_N^2 = B(C_T^2 + 2a\, C_{Tq} + a^2\, C_q^2)$$

where B is a conversion constant, a is a factor which depends upon the type of radiation propagating and C_{Tq} is the temperature-humidity co-spectrum structure parameter. The latter term characterises the correlations of temperature-humidity fluctuations. For optical propagation C_T^2 is generally the dominate term although for over water paths the C_q^2 term can contribute to C_N^2 in the IR region. The basis for the structure constants stems from spatial filtering of the correlations which fall off with separation r according to

Manuscript submitted July 27, 1982.

$$(n(x) - n(x+r))^2 = C_N^2 \, r^{2/3}$$

Although the correlations between temperature and hunidity fluctuations can add to or substract from the refractive index fluctuations the C_{Tq} term was neglected in the measurements made on the USS LEXINGTON as was C_q . The C_T structure constant is determined from the temperature difference (Δt) measured between two probes studied at a distance r apart (normally 10 to 15 cm). Once Δt) (measured in terms of an RMS voltage) is determined, it can be related to C_N^2 by

$$C_N^2 = \left(\frac{2627.5 \times P \times 10^{-6}}{T^2}\right)^2 \cdot \left(\frac{\Delta T}{r^{1/3}}\right)^2$$

where T is the air temperature in degrees K, P is the atmsopheric pressure in inches Hg and r is the probe separation in meters (= 0.10m). This method of determining C_N^2 thus neglects any contribution from humidity fluctuations.

3. USS LEXINGTON

A description of the aircraft carrier USS LEXINGTON has been reported elsewhere[1,3]. In brief, the LEXINGTON is a training carrier operating for 10-14 days in the open waters of the Gulf of Mexico. In that sense she is not a truly operational ship and only hosts fixed wing aircraft of T2, TA-4J and C-1 type. Figure 1 shows a top view of USS LEXINGTON.

4. EXPERIMENTAL EQUIPMENT

The equipment used to measure the near-ship optical turbulence is shown schematically in Fig. 2. It consisted of a Contel model MT-2 microthermal unit with modified probe system as discussed below, a RMS log amplifier, a HP 59313A

4 channel analogue-to-digital converter and a HP 9825A calculator. The output from the log amplifier was proportional to the log of C_N^2.

The original probe system provided with the Contel system[4] was replaced with the probe assembly built for use in the Harris microthermal probe system[5]. The probe wires used were 2 micrometers in diameter, half the diameter used in the previous measurements on the LEXINGTON. The probes were set 10cm apart on a wind vane which could be clamped to any suitable rail. The assembly could be mounted up to 38 meters from the control unit. Figure 3 shows a photograph of the vane assembly mounted on the starboard gun tub railing. The choice of a smaller diameter wire was twofold: firstly a number of the plug-in probes were already available and secondly the finer wires would provide a higher C_T frequency response. Digitization was done at the rate of two points/second with a time constant on the log amplifier set to 1 second. This sampling rate was limited by the HP 9825A accessing the A-D converter. The digitized turbulence data were recorded onto magnetic cassette tapes for later analysis.

Some measurements were also made of the C_T turbulence frequency spectrum in the near-ship environment. To accomplish this the output from the log amplifier was diverted to a HP3582A low frequency spectrum analyser. The resulting spectra for frequency intervals from 0-10 Hz to 0-100 Hz were then stored onto magnetic cassette tape using a HP 85 computer[6]. The system time constant chosen for these measurements was 0.01 second.

During this series of experiments contamination of the probe wires by sea-salt was considered as a possible source of error in measuring C_N^2, particularly if the relative humidity is between 80-90%.[7] However, each pair of wires was not used for any period greater than 3 hours. In most cases probe failure made it necessary to change the wires more frequently. Examination of

the unbroken used wires under magnification revealed very little deposit on the wires.

5. LOCATION OF PROBES ON LEXINGTON

During this series of measurements only one microthermal probe system was used for the three locations selected on the LEXINGTON. These locations included the forward rail on the starboard (STBD) gun tub, forward of the middle port hole in the secondary conning station (SCS) and outside the forward starboard hanger bay door. Figure 1 shows the placement of the probe system in the STBD gun tub and SCS while Fig. 4 gives the position for the probe assembly adjacent to the forward hanger bay door.

The probe position selected just outside the SCS port hole (Fig. 5) should be free from most near-ship effects except for a possible influence on C_T values due to a modified wind flow arising from the leading edge of the flight deck forward structure pointing into the wind.

At the hanger bay door the probe assembly was mounted on top of a 3.2 meter step ladder located about 1 meter from the life-guard rail on the deck. Figure 6 shows the location of the step ladder relative to the railing. This location is near beam center of the future ship-to-ship laser transmittance measurement.

6. CALIBRATION

The calibration procedure adapted for the microthermal probe system was that provided by the manufacturer, Contel. This procedure entails switching a 301 kΩ resistor across one of the probe wires at a rate of about 6 Hz. In this way a given output voltage can be related to a known value of change in probe resistance. During calibration the RMS log amplifier is maintained in the system so that the calibration factor (k) includes the gain component. After calibration the output signal can then be related to RMS (ΔT) by:

$$RMS(\Delta T) = \frac{\Delta V}{\alpha K} = \frac{\Delta V}{\alpha} \frac{R_p}{2R_c} \frac{1}{\Delta V_c}$$

where R_p is the probe resistance, R_c the internal calibration resistance, α is the thermo-resistive coefficient for the probe wires (3.50×10^{-3} $\Omega/^oC$) and ΔV_c the RMS output voltage corresponding to ΔR. Rp for the probe wires used in the measurements was typically between 56 and 61 Ω. C_N^2 can be related to $RMS(\Delta T)$ by the following expression:

$$C_N^2 = \left\{ \frac{2627.5\ Px10^{-6}}{T^2} \cdot \frac{RMS(\Delta T)}{r^{1/3}} \right\}^2$$

where T is the air temperature in degrees K, p is the atmospheric pressure in inches Hg and r is the probe separation in meters (0.1 m). Thus, the voltage output from the log amplifier is proportional to log C_N.

In the previous series of measurements[1] on the LEXINGTON 4 μm diameter wires were used on the original Contel probes. Consequently, the lower values of R_p [~ 20 Ω including 100ft cable) increased the noise figure for the whole system. Since calibration signal levels were not much higher than the noise level, it was necessary to add the signals orthogonally.

With the 2 μm diameter probe wires used in the current set of measurements the noise level was considerably reduced. Typically, log V_n = 0.1 and log V_c = 1.7. (Note that the Contel microthermal probe system was originally designed for an optimum probe resistance of 90 Ω. Decreasing R_p will lower the effective probe sensistivity as seen by the bridge and broaden the bridge balance point.) Figure 7 provides an example of a calibration run.

7. DATA ANALYSIS

C_N^2 turbulence data were recorded for periods of 8 minutes; the recording interval being limited by the storage capacity of the HP 9825A to 960 data points. Figures 8 and 9 reproduce the C_N^2 data measured at the starboard gun tub while Fig. 10 shows the data from the SCS site. All data collected during aircraft launches are shown while only a representative sample of the data are shown for the background. The figures also show the time, the type of aircraft and catapult launched from, and changes in ship's course. The type of aircraft are designated as follows:

T	T-2 "Buckeye" Jet Trainer
A	TA-4J Trainer version of A-4 jet
C	C-1 "Cod" twin engine propellar driven aircraft

The aircraft launch information was taken from various logs maintained on the ship during flight operations.

It should be noted that the scale on the left hand side of the turbulance plots represents the output of the RMS log amplifier. The calibration factor allows the C_N^2 on the right hand scale to be easily determined because of the direct proportionality between the output voltage and C_N. All figures show data plotted for 0.5 second intervals.

The data analysis has been divided into several parts. In the first instance the data have been examined and compared with the data from the 1979 experiments. Using the limited bulk meteorological data available, values of C_N^2 are then predicted and compared with the background values of C_N^2 measured. Then the influence of high C_N^2 values at the hanger door on the ship-to-ship tracker performance is examined. Finally, several frequency spectra of C_T data taken during no-launch periods are presented and analysed. The following sections will describe the results of these analyses.

8. RESULTS AND DISCUSSION

A. C_N^2 Background levels.

The first major observation made about these data is that the mean C_N^2 values during no-launch periods were at both STBD and SCS locations generally of the order of 5×10^{-15} or less except for the period 1022 to 1253 hours on 23 March where values of C_N^2 during the no-launch periods were 10^{-14} $m^{-2/3}$ or greater. This value is in good agreement with the measurements made by Horton from the STBD gun tub. In an open-sea environment an average value of $C_N^2 \simeq 10^{-15}$ $m^{-2/3}$ is regarded as being typical. It would appear that near-ship effects on C_N^2 at these two locations are minimal if the ship is steaming into the wind. The higher values of C_N^2 after 0910 hours on 23 March (Figs. 9d to 9h) are most probably explained by a small change in wind direction with the probes, measuring turbulence in air that may have passed over the flight deck and catapult. The data recorded on 23 March (Figs. 8a and 8b) reveal macro-variations with periods ranging from 1/2 to 2 minutes.
During this period the ship's course was 150^{o} and the wind direction 33^{o}. Hence, the ship was travelling not all that far off normal to a wind of 13 kts. At the ship's speed of 20 kts the data do suggest that it could have passed through macrohomogenieties with scale size of the order of 35m that occurred across the wind flow. These large scale variations were not so evident on the other two days when the ship was steaming into the wind. Alternatively, the variations in C_N^2 could be the result of an air flow oscillation being set up at that site due to the ship's movement.

B. Influence of Aircraft Launch on C_N^2

The thermal micro pulses or spikes recorded at aircraft launch in most cases peaked at a level 100 to 1000 times higher than the average background level prevailing. When the launches were made on the port catapult and C_N^2 measured at the STBD gun tub (Figs. 9a to 9d), the decay time before the C_N^2 level returned to the background level generally lasted up to 30 seconds. With launches made using the STBD catapult the decay was 15 seconds or less (Fig. 9f). Decay times measured from Horton's data for STBD catapult launc and TA-4J jet aircraft also gave values close to 15 seconds. Repeated pro wire failure when the STBD catapult was used limited the number of records two. Failure was most likely due to small grit-like particles hitting the . ile wires. The broader pulses recorded during the use of the PORT catapult indicate the wave of turbulent air has spread out by the time it has reached the STBD gun tub and therefore is taking longer to disperse. The levels of the 2 spikes recorded with STBD catapult (Fig. 9f) were noticeably higher even though the background C_N^2 was nearer 10^{-14} than $10^{-15} m^{-2/3}$. Horton in his analysis of the 1979 data provided a word of caution when interpreting the meaning of these thermal spikes. He says these spikes really do not represent true C_N^2 changes but simply represent temperature pulses of short duration. This must be regarded as the most plausible explanation until further work is done with an optical system.

The data recorded at the SCS location reveals thermal spikes peaking at times from 500 to 1000 times the background C_N^2 level (Figs. 10a to 10h). The decay time to return to the background level was the order of 30 seconds. This is expected as the probes were exposed all the time to the full influence of the aircraft exhaust which would be slower to dissipate as the ship was steaming into the turbulent air as it is formed.

C. Predictions of Background C_N^2 Using Bulk Method

Recently several papers[8,9] have been published on the verification of using the bulk method for calculating overwater optical turbulence. This method allows the readily available shipboard meteorological measurements to be used to predict turbulence over water. The theoretical understanding of the relationships involving the basic parameters is now well understood. Furthermore, the recent experiments undertaken by Davidson, et al[9] in Monterey Bay have indicated that the bulk method estimation of C_N^2 can be expected to be adequate 50% of the time where horizontal homogeneity exists on a scale of the order of 10 Km upwind. However if inhomogeneity is know to exist then the prediction can be considerably in error. This method requires only four parameters, air temperature, relative humidity and wind speed at a height z above the sea surface and the sea surface temperature. As an exercise C_N^2 was calculated using the expressions given by Friehe[2]. The bulk parameters used were taken from the ships meteorological records which had the required parameters tabulated every hour. For the wind data ($\bar{U}$) the wind over the deck readings were used. This parameter was recorded every time a launch occurred. The value of z was taken as 14 meters. Table 1 summarizes the hourly meteorological data for the times C_N^2 measurements were made. In all except one case the air temperature was greater than the sea surface temperature (i.e. $\Delta T<0$). This is conducive to stable conditions existing in this region of the atmosphere. Hence, the bulk aerodynamic formula which provides C_T^2 for stable conditions was used. This expression taken from Friehe[2] is

$$\frac{C_T^2 \, z^{2/3}}{(\Delta T)^2} = 3.12 \times 10^{-3} \, (1 - 0.635 \, X)$$

where

$$X = [(Z\Delta T/\overline{U^2})] \, \{1 + 0 \, .212 \, (\Delta q/\Delta t)$$

and

$$U\Delta T < 25.$$

The results of these calculations converted to C_N^2 are also given in Table 1. Since only hourly values were available, the same values were plotted with the experimental data $\pm$ 1/2 hour either side of the hour. These values are shown as dashed lines in Figs. 8 to 10. Apart from the period from 9010 to 1253 on 23 March the predicted C_N^2 values, surprisingly, show reasonable agreement within a factor of 3 to the mean measured C_N^2 data.

D. Turbulence Effects On Ship-to-Ship Tracker Performance

A set of measurements of C_N^2 were also made between the hanger bay door on the starboard side and the life-guard rail. Figure 6 showed the probe assembly at this location. The results of four 8 minute recordings are reproduced in Figs. 11a to 11d. At first glance these data reveal a high level of C_N^2; generally 2.5 times higher than the normal overwater value. At this location such values are expected because warm air with temperature of the order of 35° C exists in this doorway. Hence, the hotter air can mix with the cooler air outside the door to produce a strong turbulent medium. It would be

expected that this strong turbulence would not extend very far beyond the perimeter of the ship. Knowledge of the turbulence level at this location is required to determine its influence if any, on the tracking performance of the ship-to-ship measuring system. Turbulence in the beam path contributes to beam wander and spreading and hence can increase the tracking error. For the ship-to-ship system, better than 140 μradian precision tracking[10] is required if the whole laser beam is to be captured by the 60" receiver. The question now is to determine the magnitude of the extra beam wander due to the increased turbulence at the hanger bay door. The variance in beam wander (in terms of angular units) for a collimated beam with a uniform intensity profile distribution, is given by [11]

$$\langle\theta^2\rangle = \frac{2.25}{L^2}\int_0^L b(z)^{-1/3}\, C_N^2(z)\, (L-z)^2\, dz$$

where b(z) is the radius of the beam at distance z. If it is assumed that b(z) and $C_N^2(z)$ do not vary significantly with z then the variance is given by

$$\langle\theta^2\rangle = 0.75\, b(0)^{-1/3}\, C_N^2\, L$$

If one divides a 5 km path into three segments such that $C_N^2 = 10^{-12}\ m^{-2/3}$ for the first 25 m, $C_N^2 = 10^{-13}m^{-2/3}$ for the next 25m and $C_N^2 = 10^{-14}m^{-2/3}$ for the remainder of the path and assuming all 3 individual values add up orthogonally then $\langle\theta^2\rangle$ can be computed for each segment to give the RMS beam wander as

$$\sqrt{\langle\theta_T^2\rangle} = \sqrt{(25.0 + 2.6 + 50.4)} \times 10^{-12}$$

$$= 8.8\ \mu\text{radian.}$$

The radius of the collimated beam was assumed to be 0.41m. Considering that the above calculation is for a very extreme case, the increase over the situation where $C_N^2 = 10^{-14}\ m^{-2/3}$ for the whole 5 km path is only 1.7 μradian. In reality, the increase in beam wander would be much less than this because the value of $C_N^2 = 10^{-12}m^{-2/3}$ would extend very little beyond the ship's perimeter. However, what really is more important to take into account is the straight out refractive effect that the large temperature change near the doorway would have in deflecting the beam since this distinct temperature change will produce a step change in the refractive index of the air. Hence, by applying Snell's law, the angular change can be determined. At $\lambda = 3.8$ μm the refractive index of air at temperatures of 30° C and 15° C is 1.00025906 and 1.00027273, respectively. Now if small angles are considered, i.e. the refractive index boundary is close to normal to the beam then $n'\nu = ni$ where n and n' are the refractive indices of air for 30° C and 15° C, while i and ν are the incident and refracted angles, respectively. This results in an angular change of about 14 μradians. Since this boundary would be fluctuating with time the angular change in beam wander would also fluctuate. The deflection calculated above represents a maximum value. Thus, as might be expected, this hot air "curtain" has a much greater effect on beam wander than the turbulence generated near the doorway. The hot air coming from inside the hanger bay (the steam reservoirs for the starboard catapult just inside the doorway contribute most to heating the air) that forms this "curtain" could be considerably reduced by having a screenplaced between the doorway perimeter and the tracker van.

In Fig 12b note that the change in ship course has produced a marked decrease in C_N^2. Prior to the change in course the atmosphere in this location was in full sunlight while after the change the area was shaded by the ship's

deck. Whether or not the absence of direct sunlight brought about a reduction of C_N^2 is difficult to say. It could also be due to a change in the movement of air along the ship. Horton in his analysis reported slow changes in C_N^2 after the ship changed course and attributed this to possibly some large oscillation of the air flowing slowly along the ship.

E. Frequency Spectra of Microthermal Fluctuations

During the C_N measurements made on board the LEXINGTON the opportunity was taken to record several low frequency spectra of the two point differential temperature fluctuations (ΔT) (see Section 4). Figures 13a, b and c show spectra that were recorded during no launching at the SCS location. In Fig. 13 the fall off in output for frequencies less than 2Hz is due to the frequency analyser. Even though AC coupling had to be used to remove a large DC offset from the microprobe output, the frequency response still remains very flat above 2Hz. Reproduced in Fig. 13d is a frequency spectrum when the probe wires are capped. This spectrum indicates a fairly flat frequency response above 5Hz. (The spectrum analyser in this case was DC coupled to the microthermal probe system which accounts for the large excursion near 1Hz.)

The Kolomogorov or inertial-subrange model predicts that the exponent in the RMS frequency spectra power law should be -5/6. Values deviating from -0.83 indicate a departure from the Kolomogorov spectrum. Now in many cases, particularly if turbulence is strong, it is found that $f^{-0.83}$ will hold for the lower portion of the spectrum but depart significantly at frequencies, say above 50 Hz.[12] A break point along the power law curve allows a value for the inner scale to be determined. Strictly, turbulence spectra should be measured using only a single microthermal probe and these spectra be studied for power-law behavior. Hence, the RMS ΔT fluctuation frequency spectra presented here will provide only a guide to the actual power-law behavior;

partial or complete cancellation of signals from the 2 probes can occur and the probe separation of 10cm limits the extent of the spectrum. Examination of the slopes (Fig. 14) determined from the curves fitted to the spectra measured on the LEXINGTON when they were plotted on a log-log scale, indicate small changes at 10 and 25 Hz. The slopes for the spectral region below 10 Hz were 1.0 (Figs. 13c and 14b) while for the region 10 to 25 Hz they were 0.5 and 1.4 and for greater than 25 Hz (Fig. 14a), 1.15. These values of the slope indicate that when these measurements were made (for constant wind and significant data averaging), departure from the Kolomogorov 5/6-law is implied. This may follow from the fact that turbulence conditions at the time were not strong and the turbulence was influenced by the location of the probes close to the ships structure. Furthermore, the model is known [12] to be more realistic under strong turbulence. However, in view of the existence of an error of unknown magnitude arising from using 2 probes to measure the spectra, this conclusion must be regarded as only tentative. The establishment of any inner scale dimension from the data in Fig. 14 was thus not possible.

Several frequency spectra were recorded during aircraft launches but no noticeable change was observed in the frequency spectra after the initial ΔT impulse was recorded by the microthermal probes.

Notwithstanding the above, the usefulness of the ΔT fluctuation spectra are limited. One use which could be seen for this type of data is to determine the degree of contamination that the probe wires receive from salt deposit in a maritime environment. Contamination of this nature will drastically reduce the frequency response and increase the ΔT readings. A frequent check on the frequency response would give the build up of contamination on the wires.

9. CONCLUSIONS

The data reported here made a small but worthwhile contribution to the data base for the nearship effects on optical propagation. In the first instance the data recorded with microthermal probes has confirmed the presence of strong thermal impulses immediately after launch at the starboard gun tub site. As referred to in an earlier section these impulses could possible be due to a thermal spike and not to turbulence. It is highly unlikely that in the short space of time after the launch an equilibrium situation would exist. One interesting aspect to emerge from ths analysis is the modest agreement seen between a majority of the measured background C_N^2 data and that predicted from the bulk parameters. Provided homogeneity is known to exist upwind the bulk parameterization method for determining C_N^2 can be used to predict C_N^2 with moderate accuracy.

At the hanger bay door very high values of C_N^2 were found to exist. However the C_N^2 value would be expected to drop very quickly once outside the ship's perimeter. Calculations using the extreme value measured for C_N^2 only slightly increased the RMS laser beam wander for the ship-to-ship tracker. However, a greater effect on the beam wander would occur from the straight refractive effect when such a distinct drop in air temperature is encountered by the beam. However, the estimated bending in the beam of 15 μradian fell well within the 140 μradian tracker pointing accuracy limit set for beam wander and spreading.

Unfortunately due to the short period on board the LEXINGTON, insufficient time was available to collect C_N^2 data at any of the aft sites, as was done for the set of measurements in 1979. If further measurements are made on the LEXINGTON using both optical and microthermal probe systems then these sites need to be included.

10. RECOMMENDATIONS

The measurements of C_N^2 made to date on the LEXINGTON have provided an insight into some of the effects the ship's environment has on optical turbulence. These data provide the basis for planning future measurements of near ship optical turbulence using optical instrumentation. There is the requirement to design a compact, portable optical system with say a physical pathlength of 1 to 2 m which can make turbulence measurements at a point location. A modified open, White cell system that can accept an almost-collimated laser beam, combined with a suitable TV or IR recording camera, could be a possible candidate for such measurements. It is essential in any such folded system that the beam be as nearly collimated as possible. For any focussing of the beam within the cell would lead to difficulty in interpreting the effects of turbulence on beam wander and spreading recorded at the exit. Even so, there still remains the problem of how to intepret the results when a beam passes through the same irregularities, say 100 times. This must be seen as a major limitation to using a multiple pass co-axial optical system. Alternatively, an an optical system based on the Schlieren method could be adopted to record beam turbulence. In this situation an almost parallel beam of non-coherent light would only pass through the same irregularities once or twice depending on the configuration adopted. Furthermore, a Schlieren system should be able to be designed to measure turbulence radially about the system's axis for a large crossectional volume using a point source. Any optical system which is used in a maritime environment will have practical problems. For example, increased scatter of the beam will occur after reflection at the mirrors as they become coated with salt, contributions will be made to beam scatter by the aerosol and, in the

case of the Schlieren method achieving overall mirror stability.
In the case of the first two effects, operating at longer wavelengths (IR) will reduce the severity of the scatter problem.

The measurement of the direct influence of turbulence on optical beams immediately takes into account the effects of temperature and humidity fluctuations and the interaction between the two, on refractive index. In the maritime environment humidity fluctuations are known to play an important role for propagating IR beams. Furthermore, the spatial filtering imposed by a two probe microthermal probe system would be removed. If a He:Ne laser is used a larger region of the sub inertial range can be covered assuming the inertial sub-range model criteria apply; the lower limit using a He:Ne laser and a 100 m path would be about 8 mm. An optical system would also provide a better understanding of the effects on turbulence of the large temperature fluctuations observed during aircraft launch. It would be advantageous then to make microthermal fluctuation measurements concurrently with measurements of optical turbulence.

ACKNOWLEDGMENTS

The author is indebted to the crew of the USS LEXINGTON for their support in providing facilities to allow these measurements to be undertaken. Special thanks must go to Dr. G. Trusty, Dr. D. Leslie and Dr. P. Lebow for providing technical and computer programming assistance during the preparation for these experiments.

TABLE 1.

SUMMARY OF METEOROLOGICAL PARAMETERS DURING MICROTHERMAL PROBE MEASUREMENTS

Date	Local Time	T_{air} (°C)	T_{water} (°C)	Relative Humidity (%)	Wind Speed (m/s)	Wind Over Deck (m/s)	C_N^2 $m^{-2/3}$)
3/22	1555	24.4	21.1	78	6.8	N/A	1.1×10^{-14}
	1655	24.6	21.1	80	7.3	N/A	7.2×10^{-15}
	1755	24.6	21.1	81	5.7	N/A	7.3×10^{-15}
3/23	0655	24.1	24.4	90	3.1	9	4.3×10^{-17}
	0755	25.6	"	81	3.1	14.5	7.6×10^{-16}
	0855	25.6	"	78	5.7	14.5	7.6×10^{-16}
	0955	25.6	"	74	2.6	14.5	7.5×10^{-16}
	1055	25.6	"	74	2.6	N/A	7.5×10^{-16}
	1155	25.8	"	78	2.1	13.5	1×10^{-15}
	1255	26.7	"	67	2.1	13.5	2.8×10^{-15}
	1355	26.6	"	71	2.6	13.5	2.6×10^{-15}
	1455	26.3	"	71	3.1	13.5	1.9×10^{-15}
	1555	26.1	"	72	1.6	12.5	1.5×10^{-15}
	1655	26.1	"	70	1.0	11.5	1.5×10^{-15}
	1755	26.0	"	70	0	13.0	1.4×10^{-15}
3/24	0755	25.4	24.4	82	5.2	14.5	
	0855	26.2	"	81	5.2	14.5	1.7×10^{-15}
	0955	26.2	"	78	6.2	13.5	1.7×10^{-15}
	1055	26.6	"	77	6.2	14.5	2.6×10^{-15}
	1155	26.7	"	78	6.8	14.5	2.9×10^{-15}
	1255	30.1	"	58	6.8	14.5	1.9×10^{-14}
	1355	27.9	"	66	6.8	13.5	6.8×10^{-15}
	1455	28.4	"	66	4.2	15.5	8.7×10^{-15}
	1555	28.4	"	66	3.1	13.5	8.9×10^{-15}

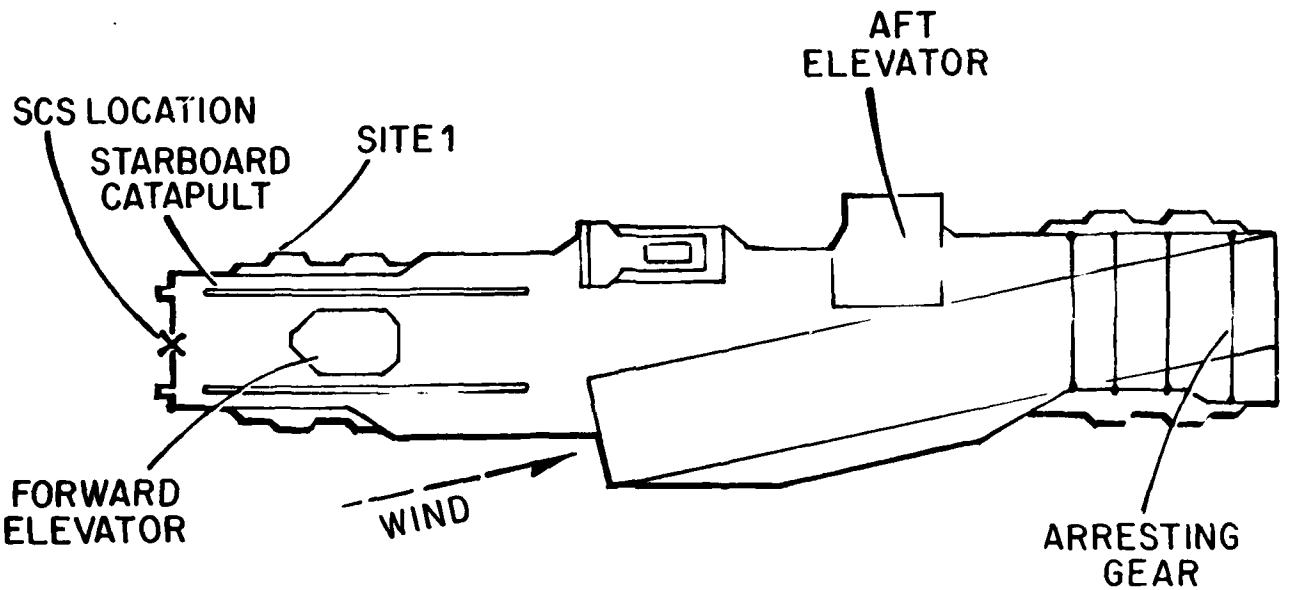

Fig. 1 – Top view of USS LEXINGTON

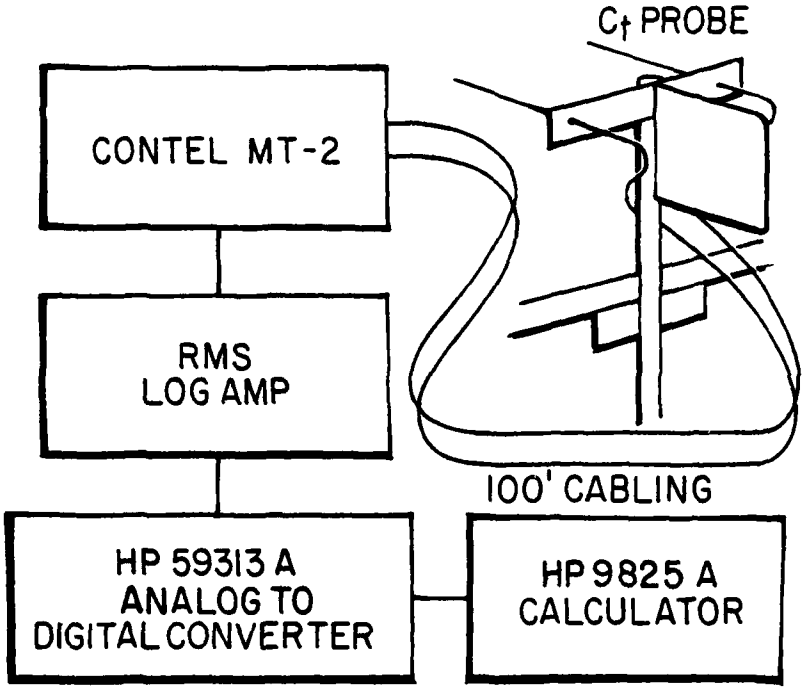

Fig. 2 – Schematic of microthermal probe system and data acquisition system

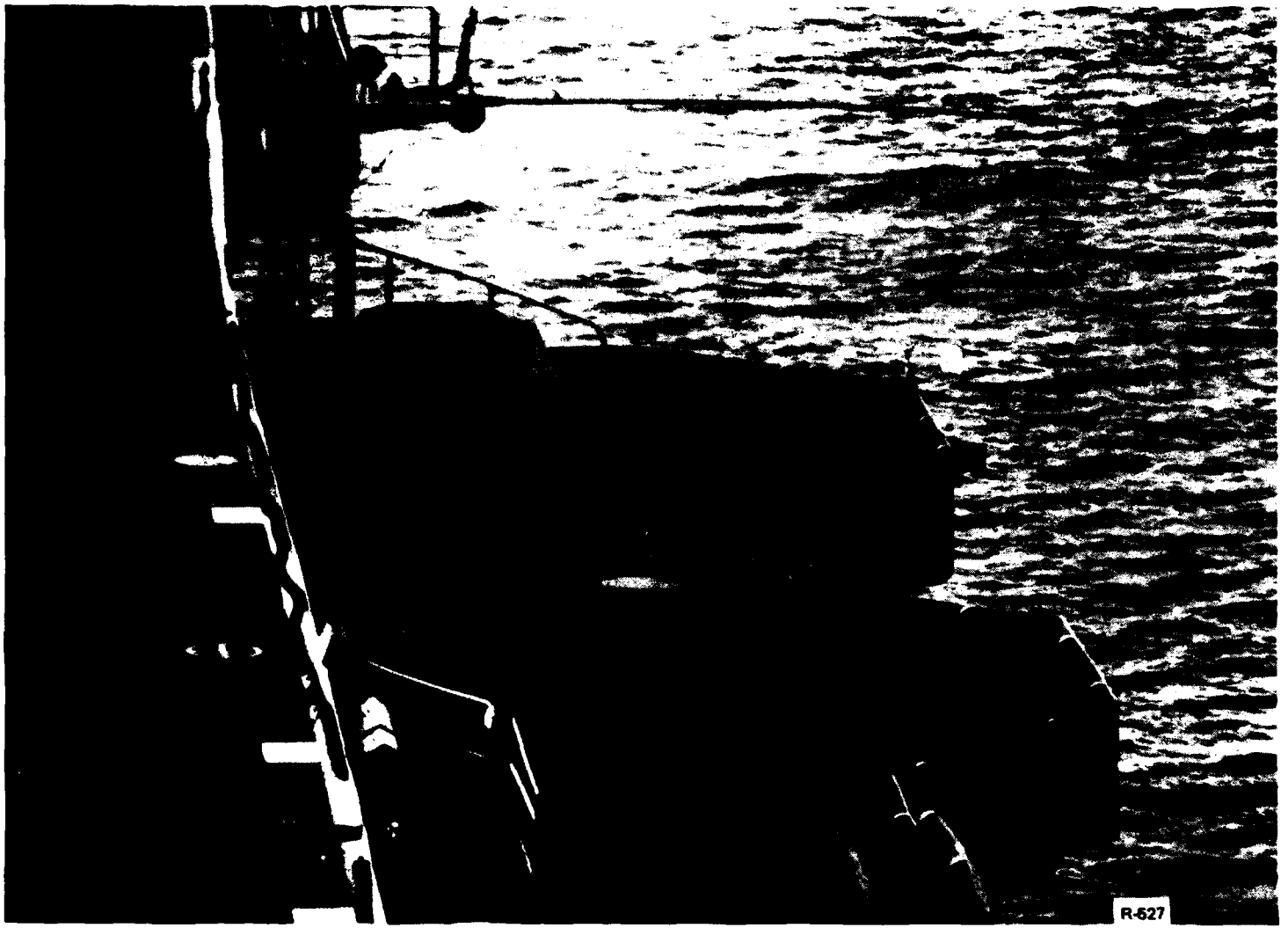

Fig. 3 – Probe assembly located on starboard gun tub

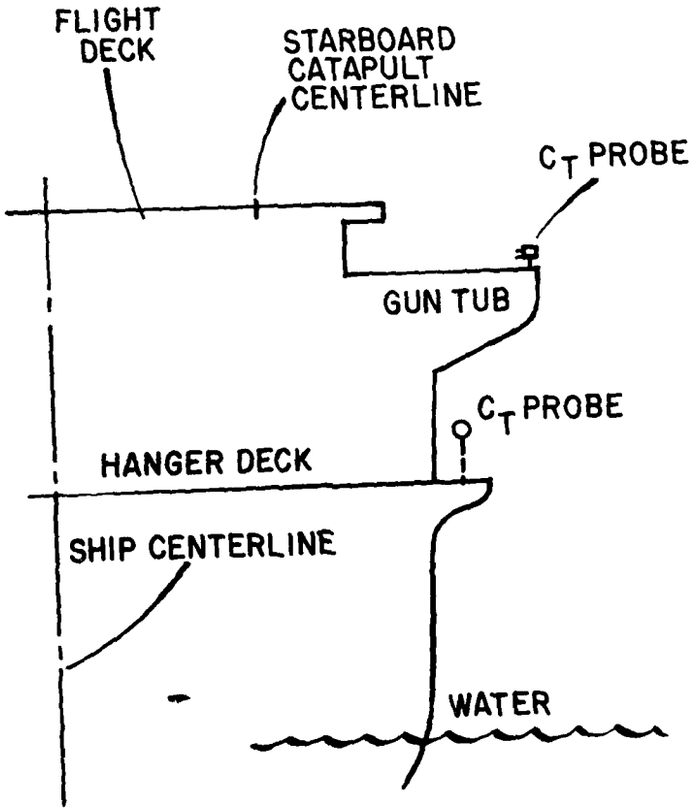

Fig. 4 — Schematic of starboard half of ship showing placement of microthermal probes at two locations

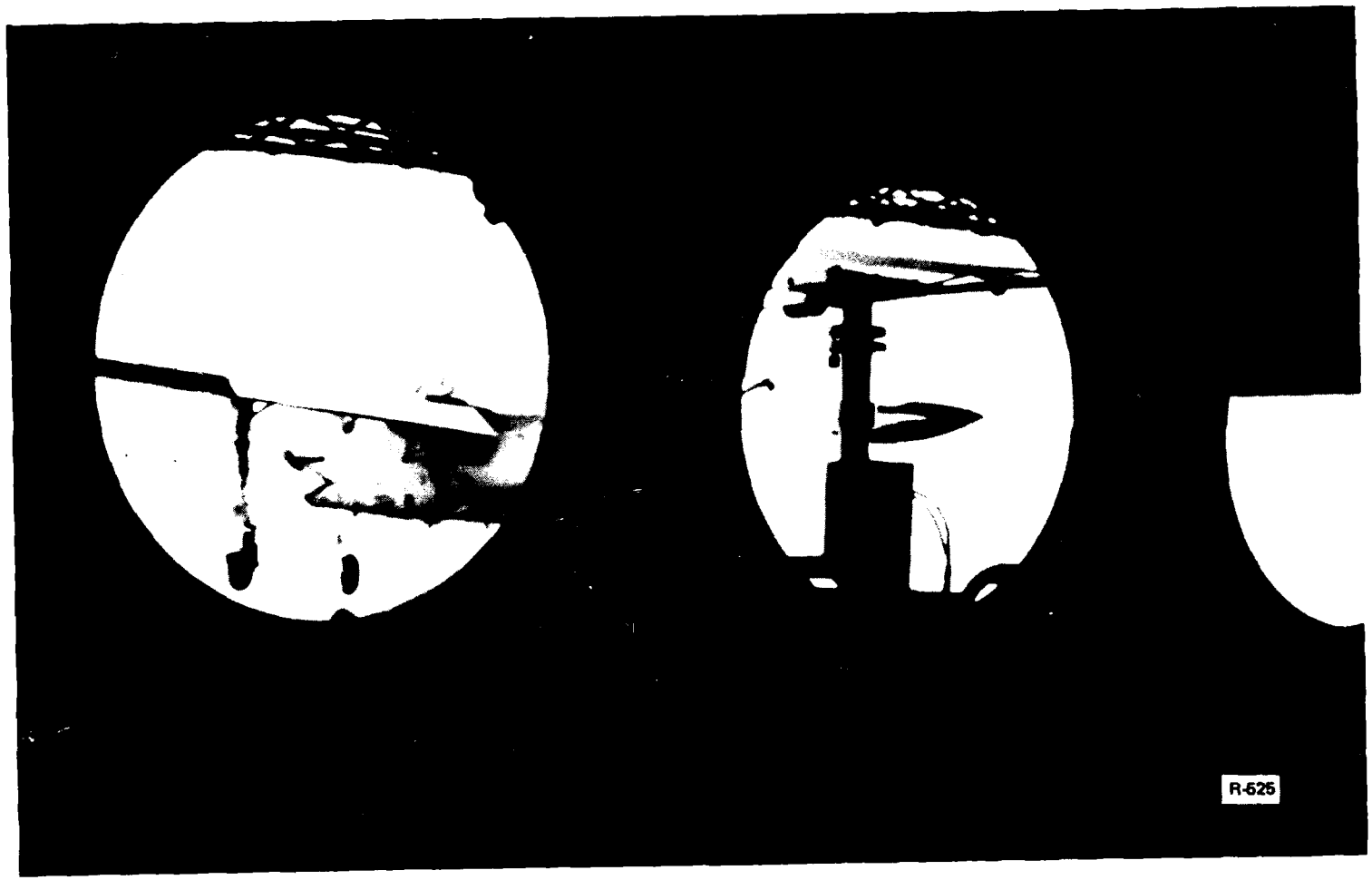

Fig. 5 — Probe assembly located at secondary conning station (SCS)

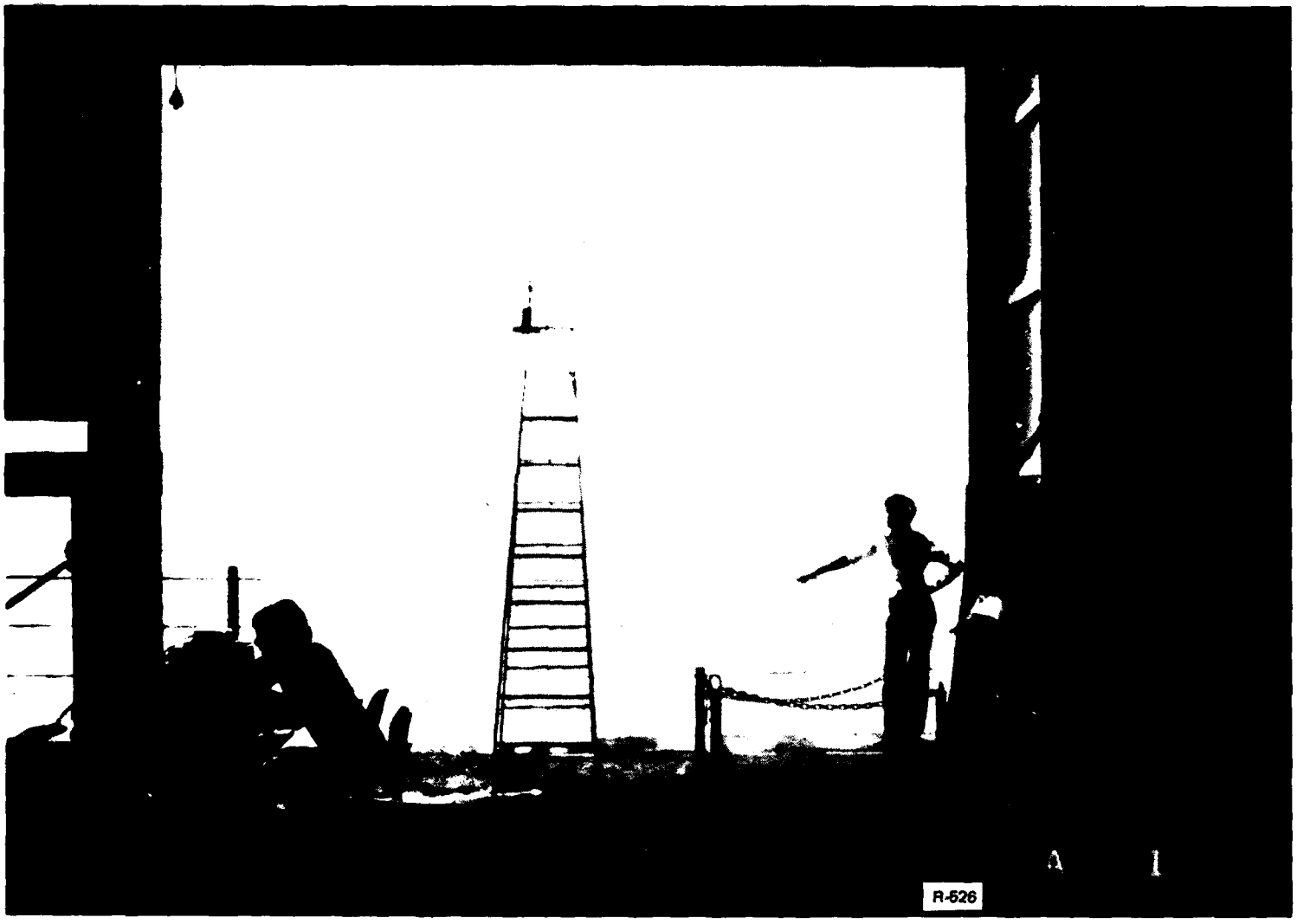

Fig. 6 – Probe assembly located at forward hanger bay door

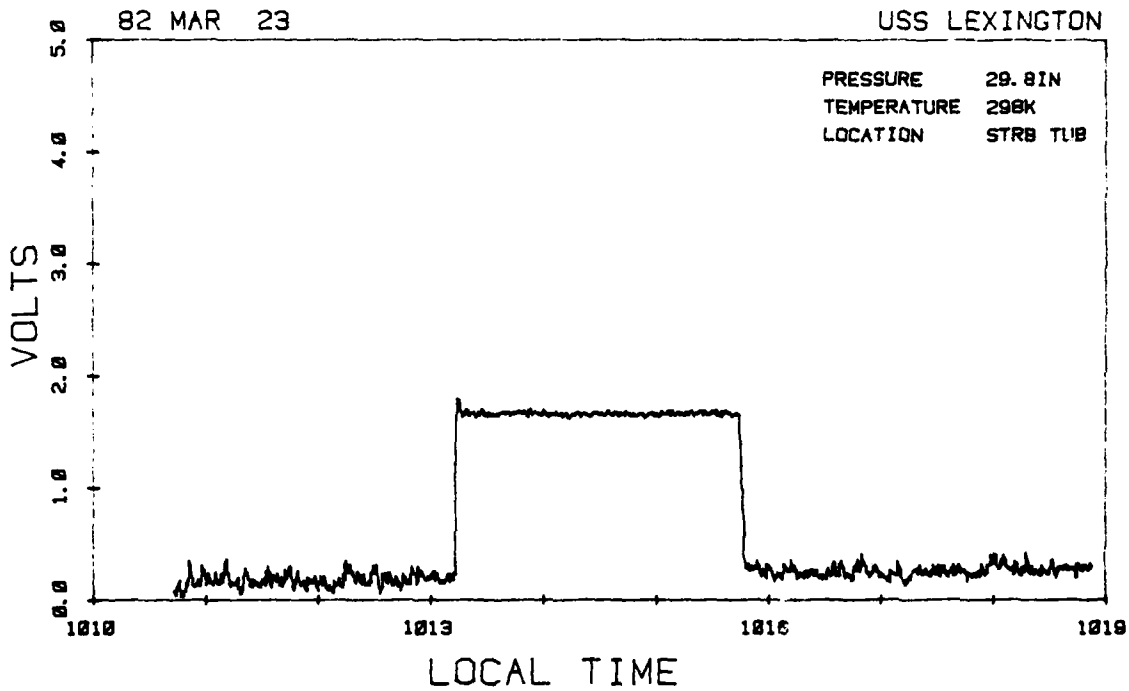

Fig. 7 — Example of a record for calibrating the microthermal probe system

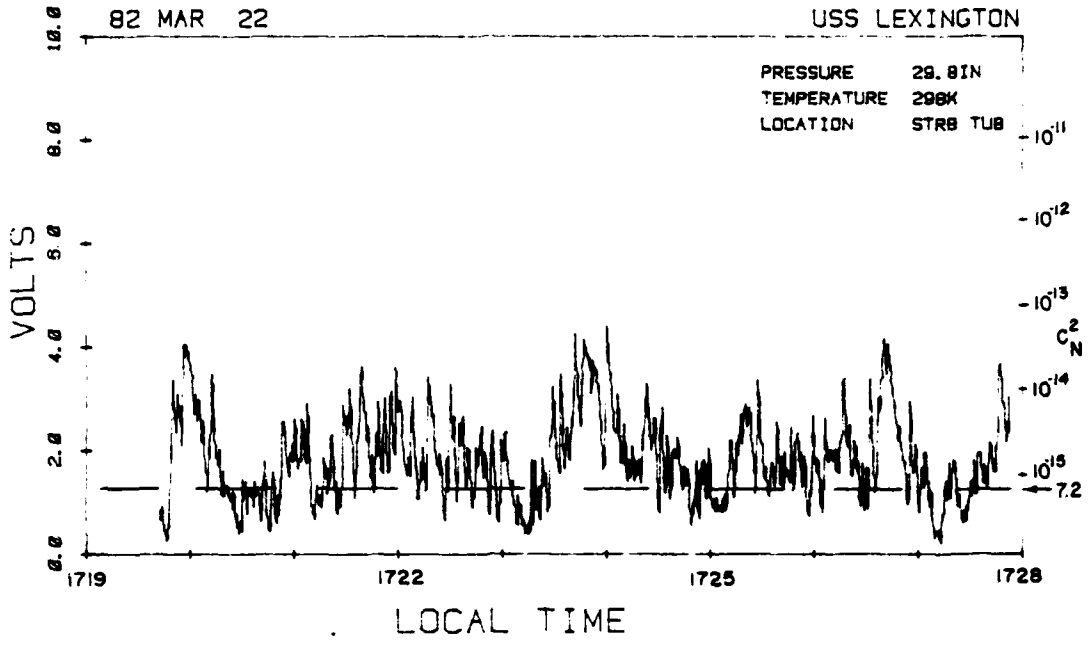

(a)

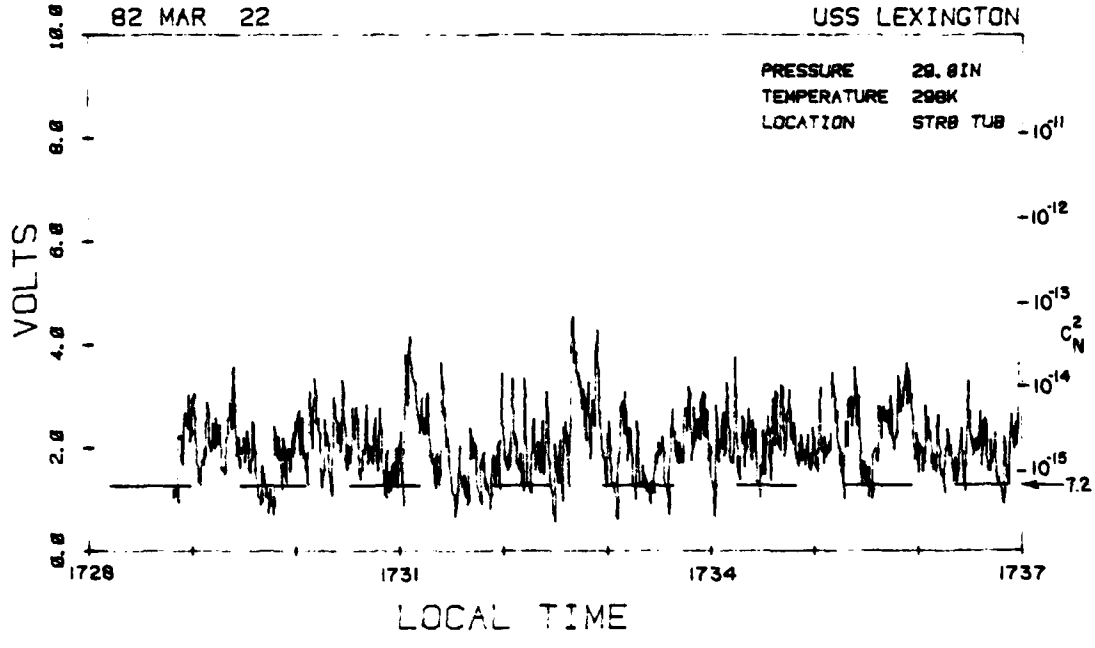

(b)

Fig. 8 — Microthermal probe response at starboard gun tub from (a) 1720 and (b) 1729 hours on 22 March

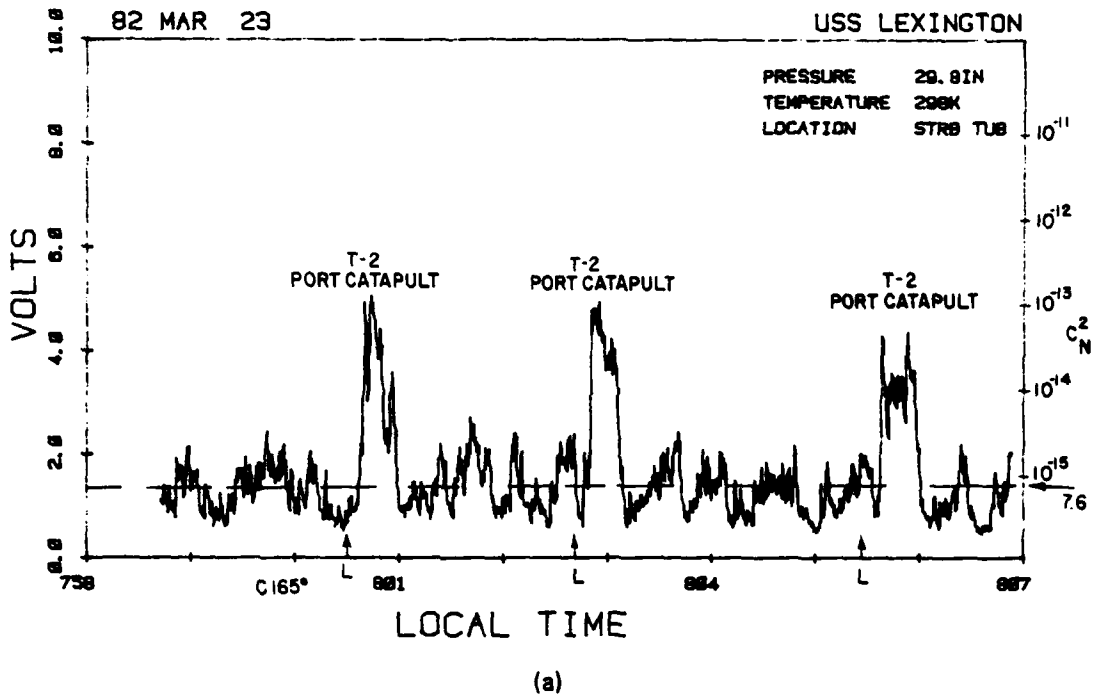

(a)

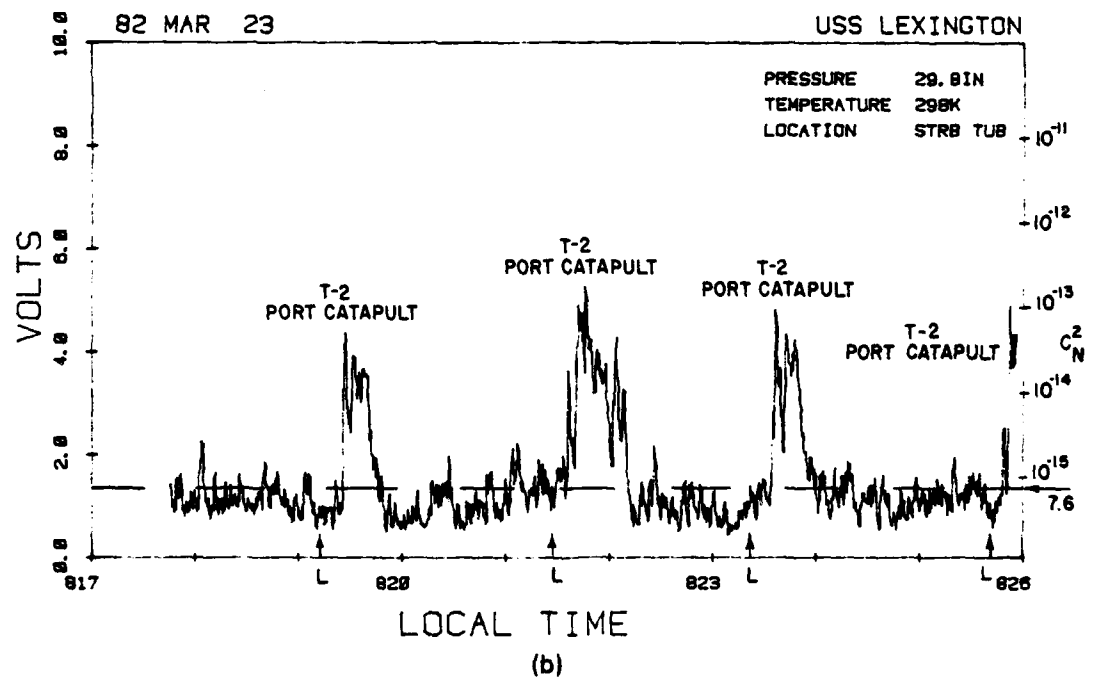

(b)

Fig. 9 — Microthermal probe response at starboard gun tub location from (a) 0759 and (b) 0818 hours on 23 March

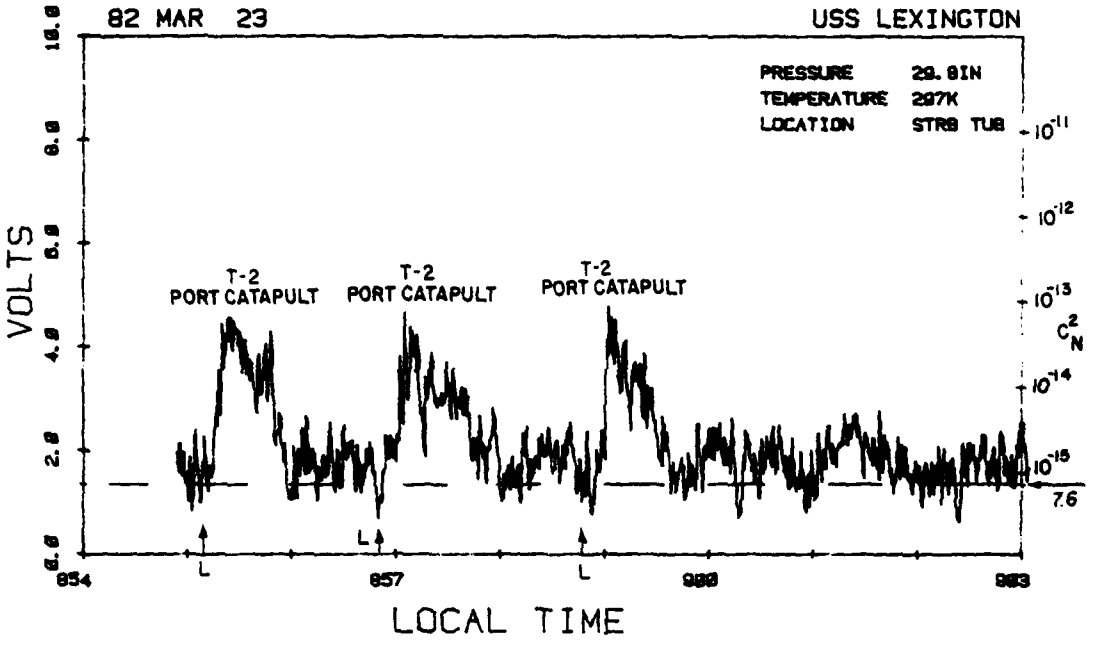

(c)

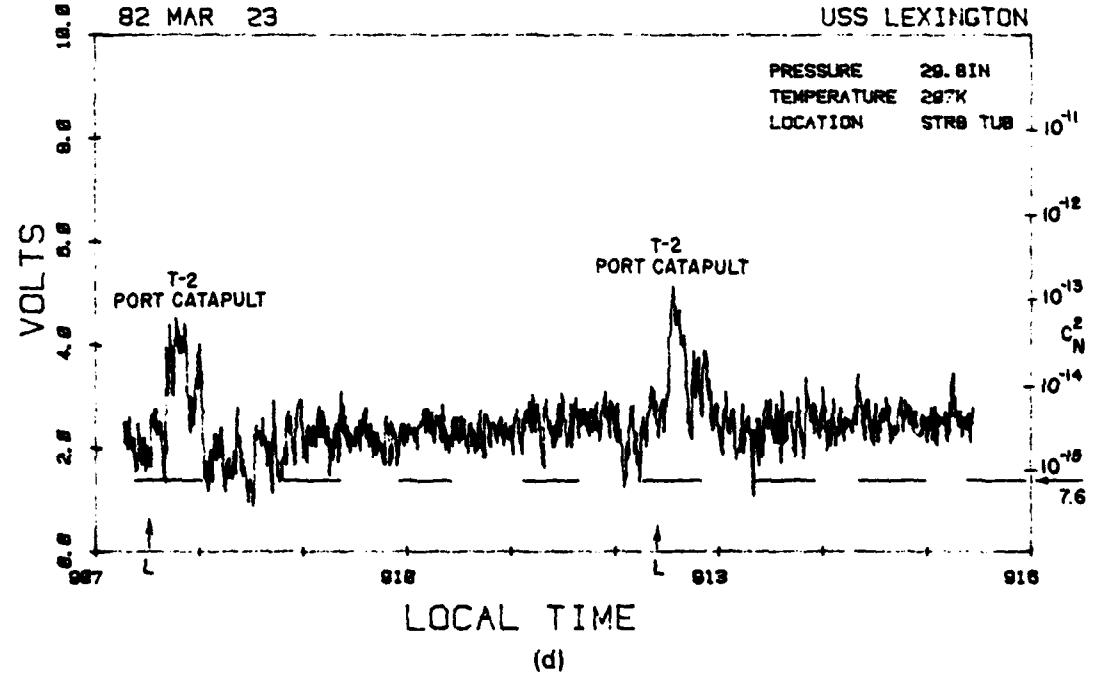

(d)

Fig. 9 — Microthermal probe response at starboard gun tub location from (c) 0855 and (d) 0907 hours on 23 March

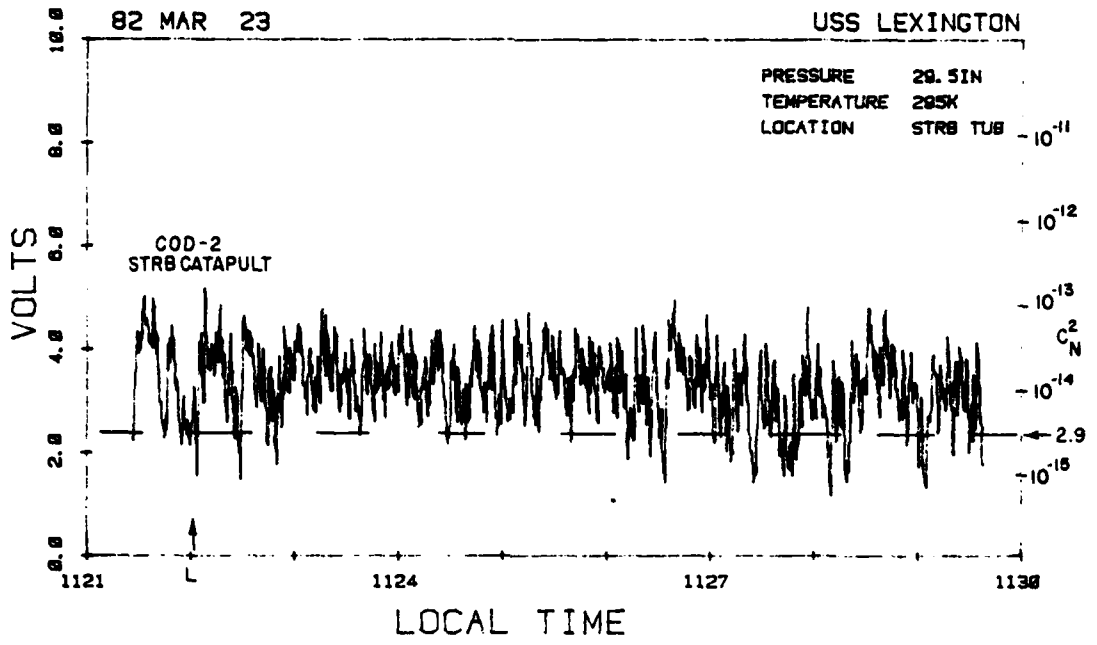

(e)

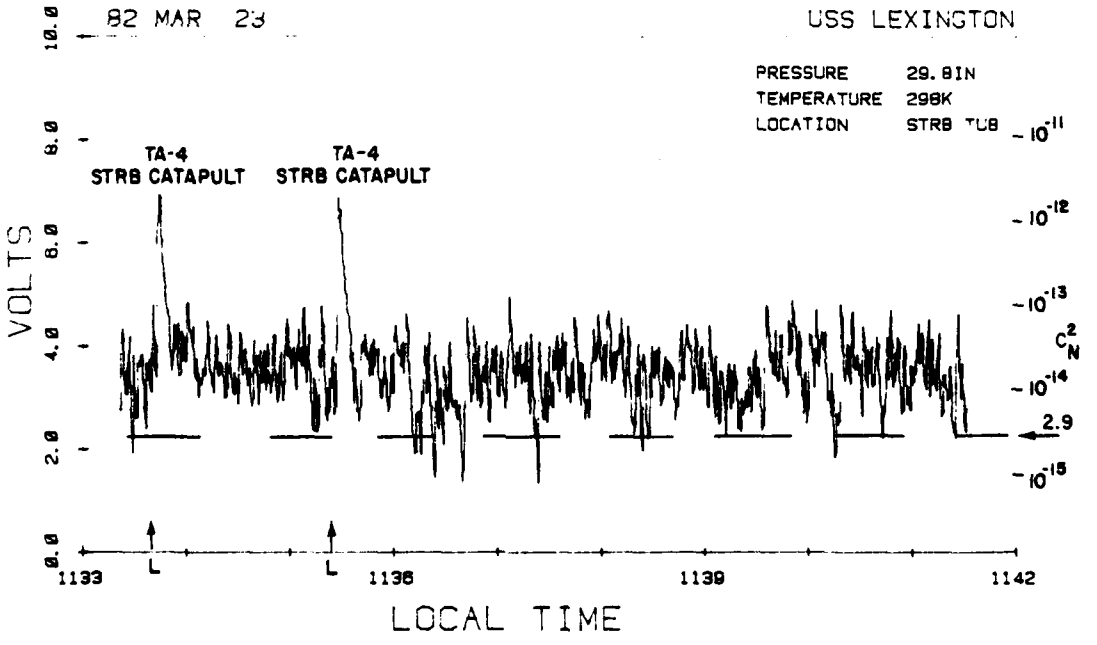

(f)

Fig. 9 — Microthermal probe response at starboard gun tub location from (e) 1120 and (f) 1133 hours on 23 March

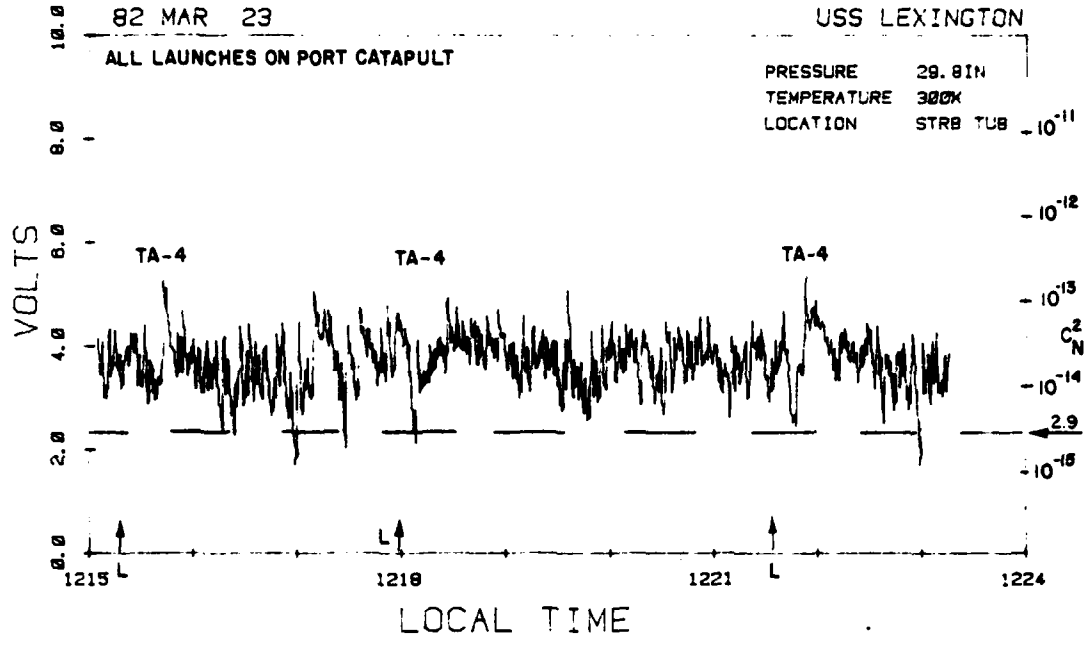

(g)

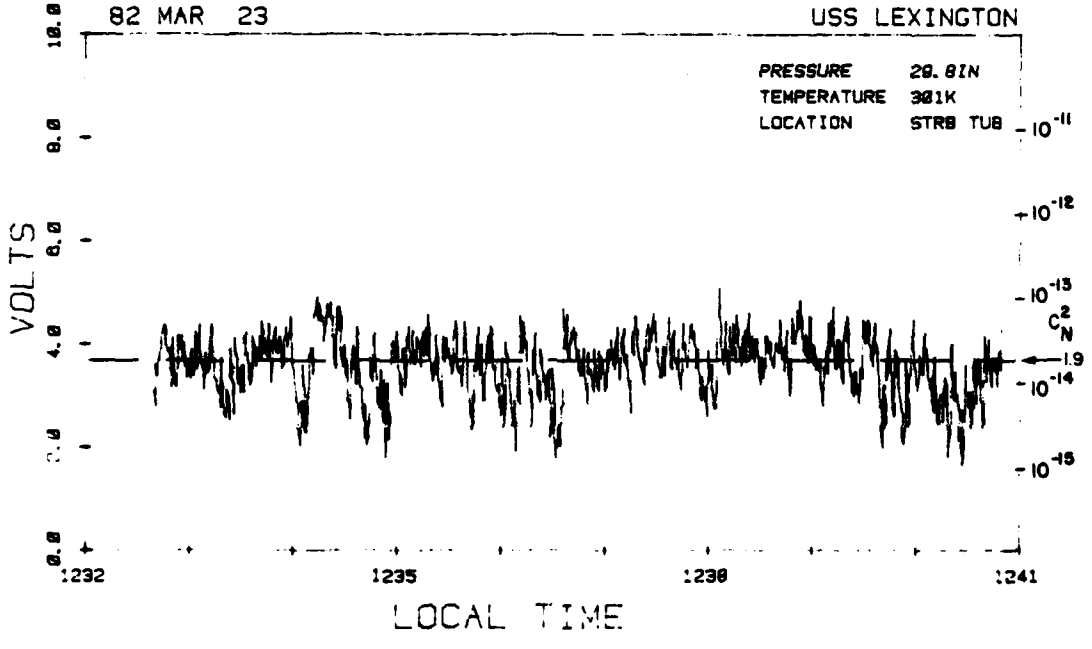

(h)

Fig. 9 — Microthermal probe response at starboard gun tub location from (g) 1215 and (h) 1233 hours on 23 March

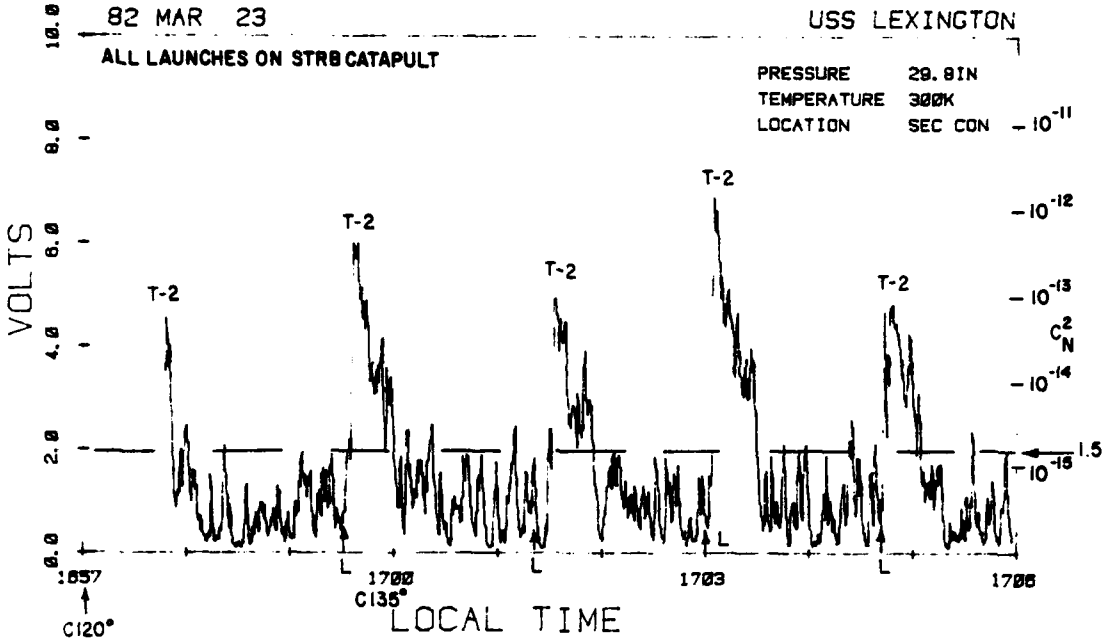

(a)

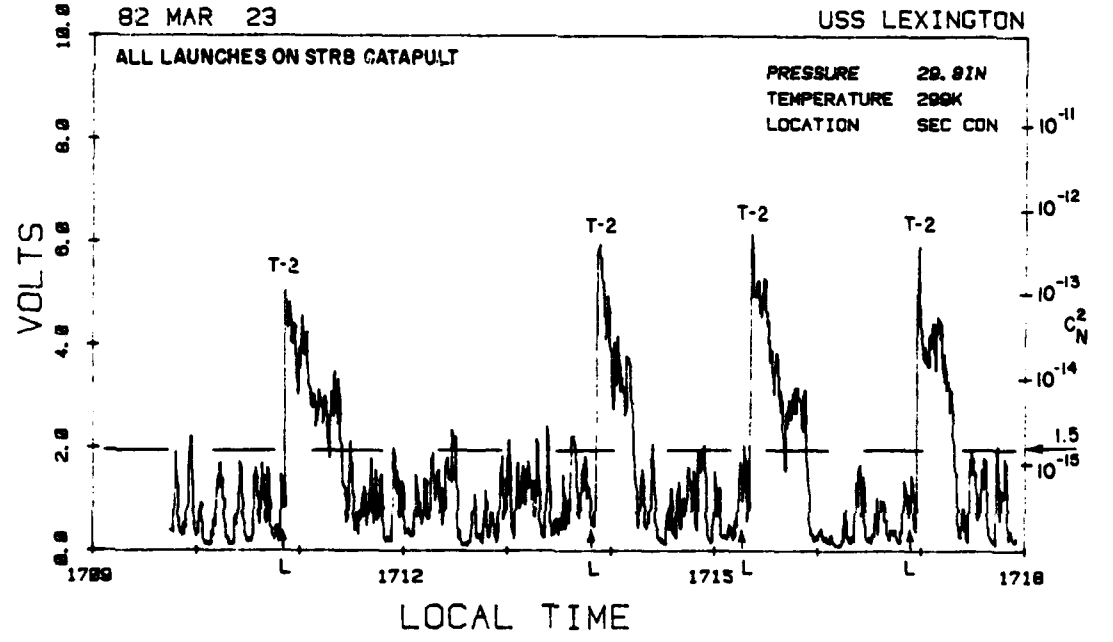

(b)

Fig. 10 – Microthermal probe response at SCS location from (a) 1658 and (b) 1710 hours on 23 March

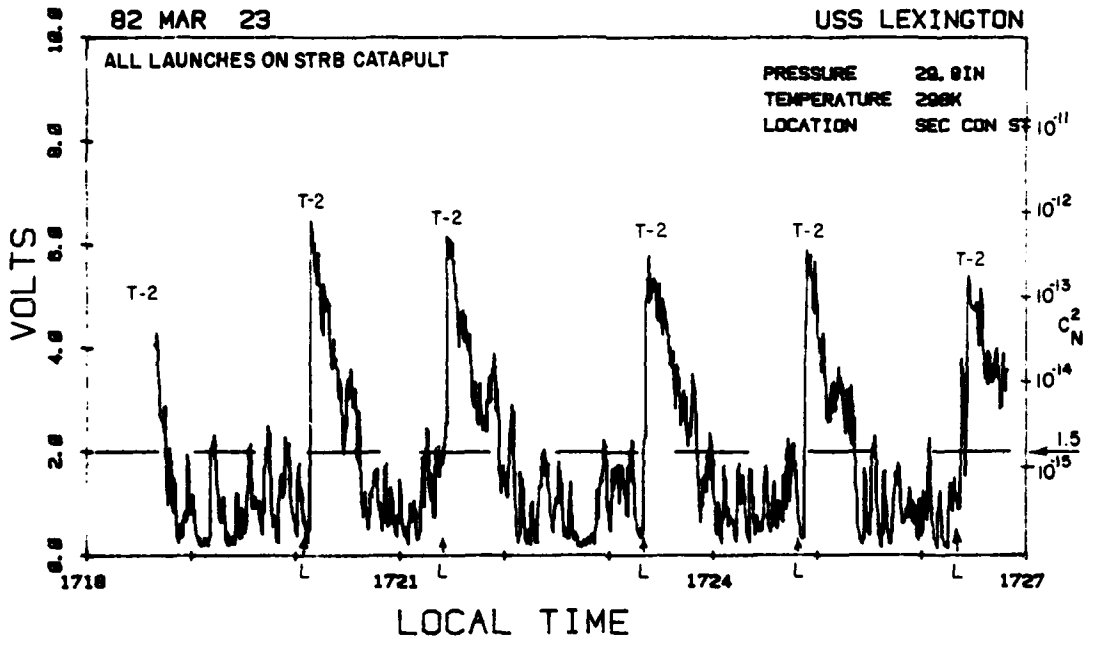

(c)

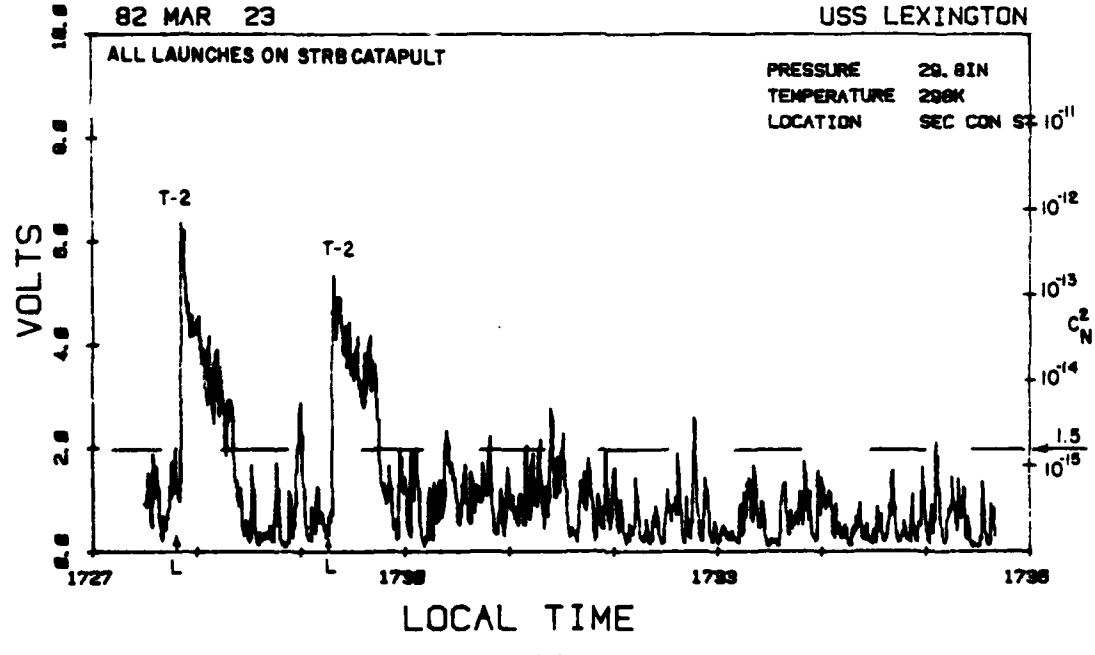

(d)

Fig. 10 – Microthermal probe response at SCS location from (c) 1719 and (d) 1727 hours on 23 March

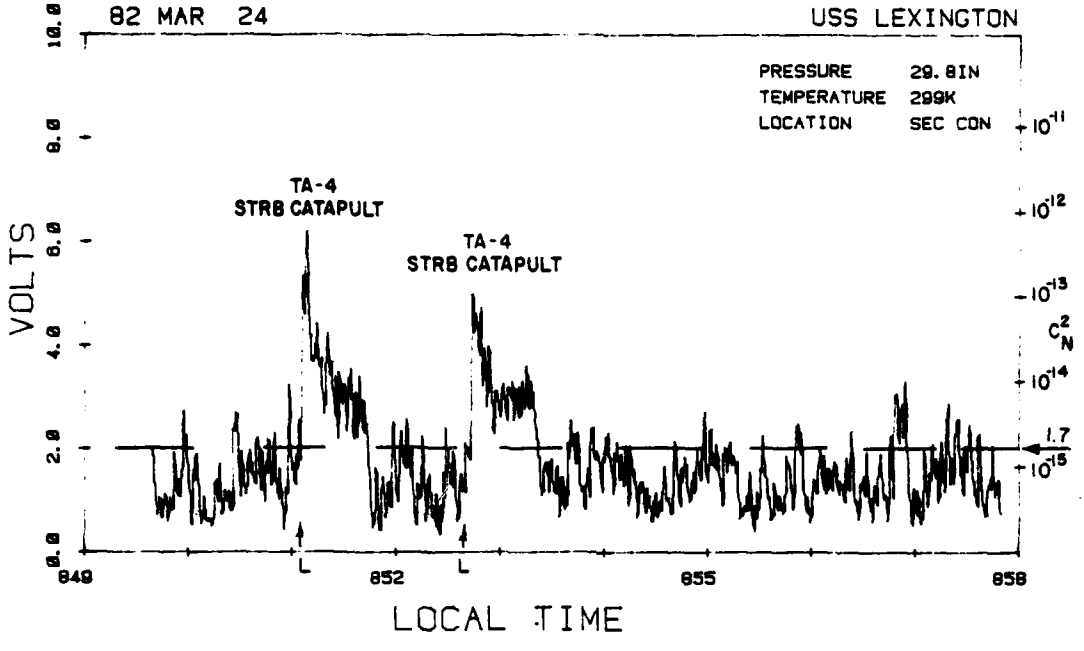

(a)

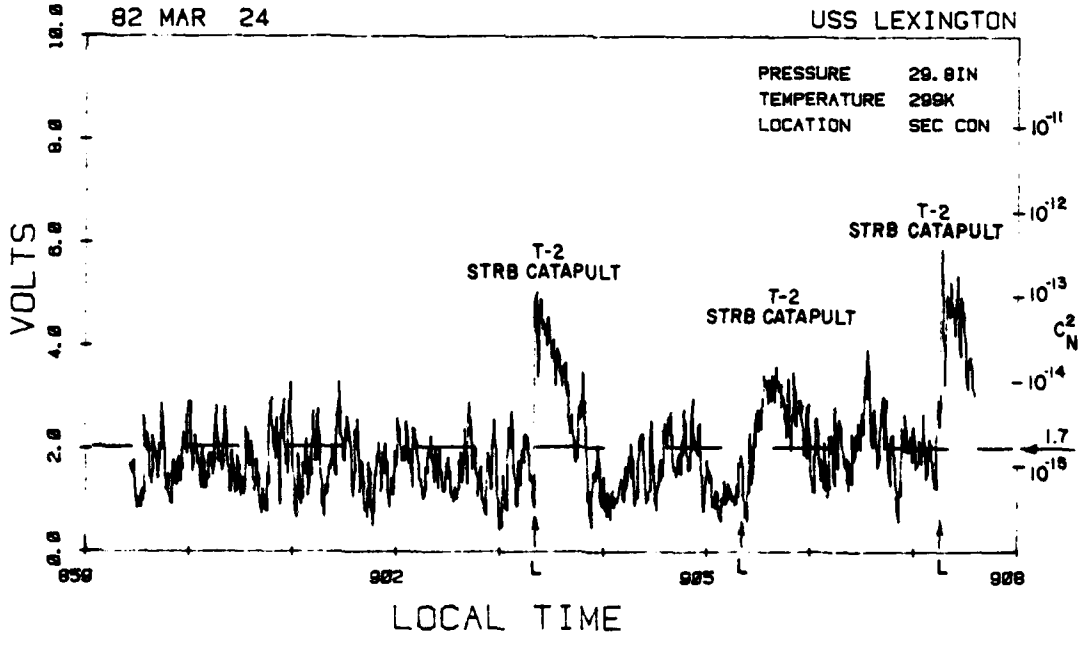

(b)

Fig. 11 – Microthermal probe response at SCS location from (a) 0850 and (b) 0859 hours on 24 March

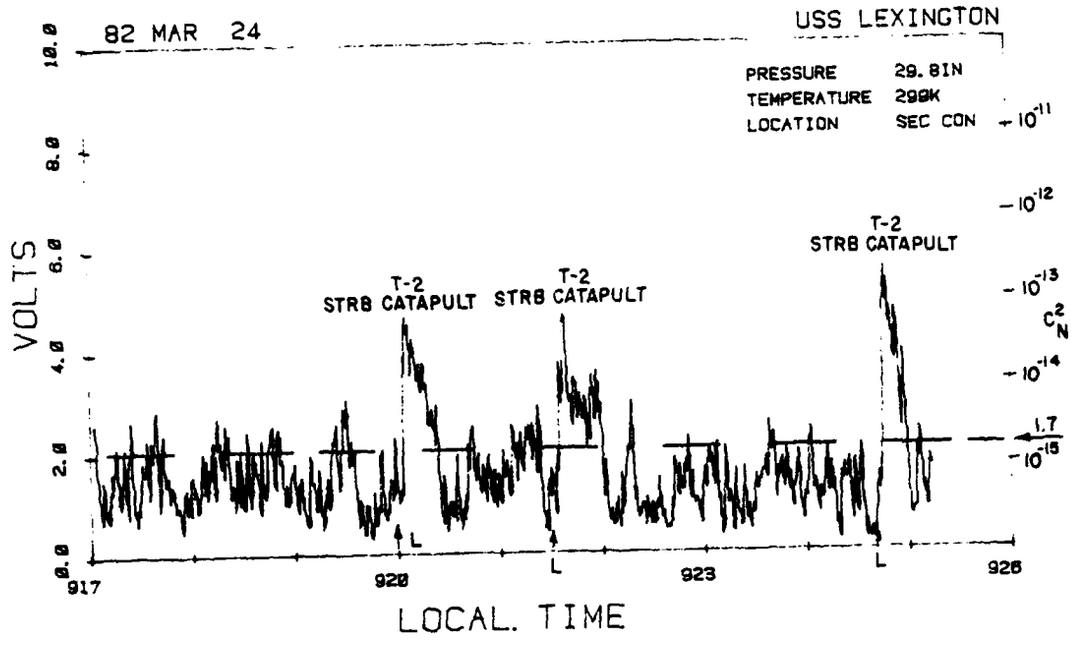

(c)

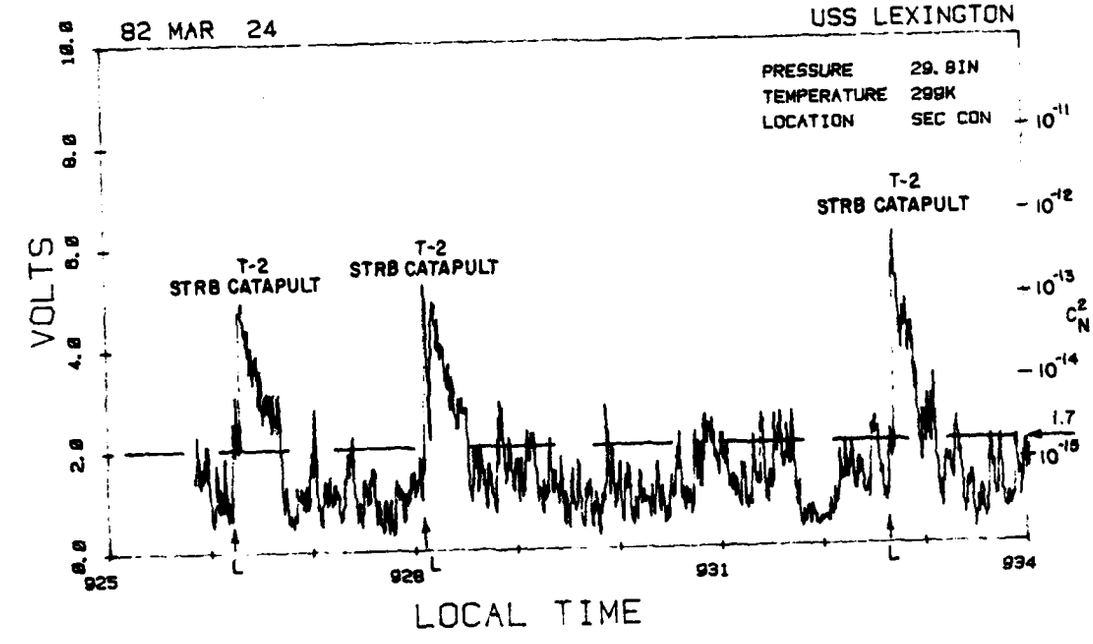

(d)

Fig. 11 — Microthermal probe response at SCS location from (c) 0917 and (d) 0926 hours on 24 March

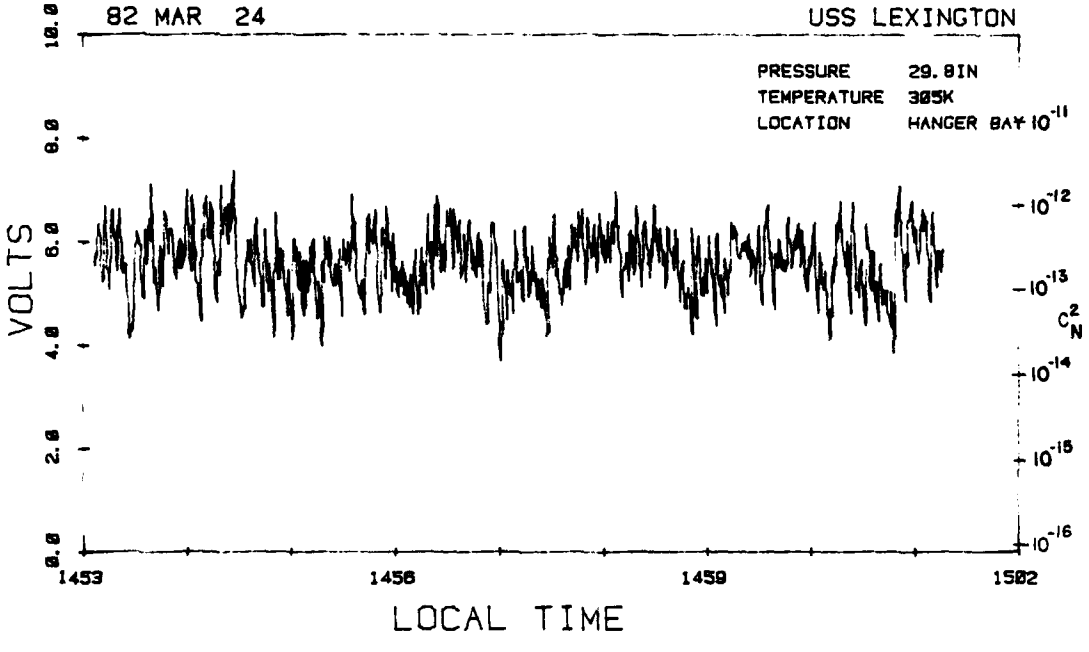

(a)

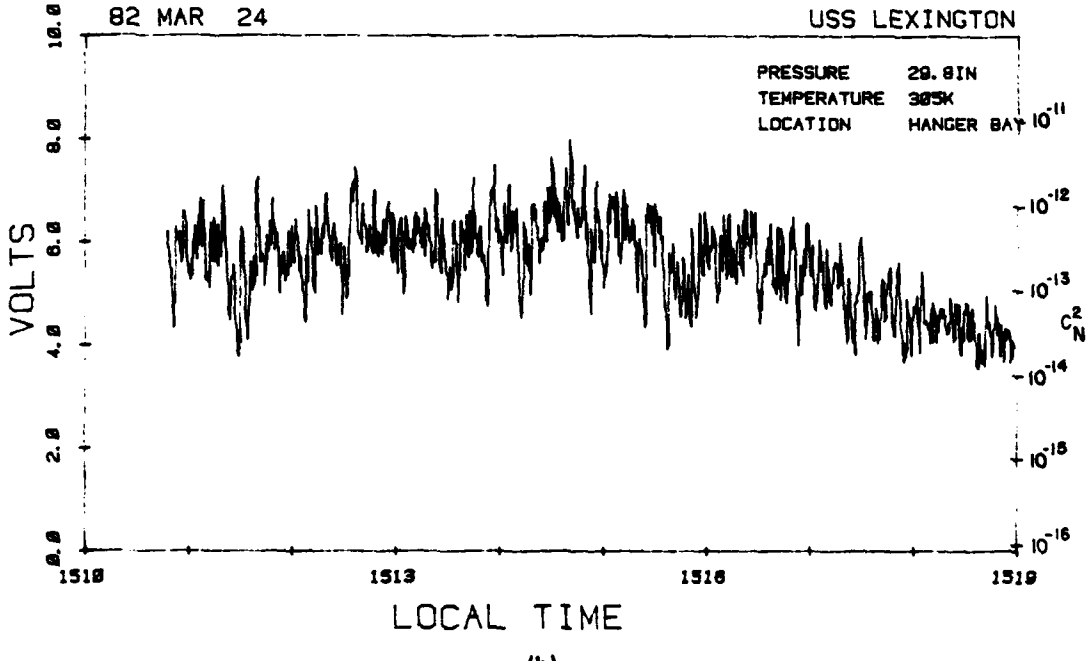

(b)

Fig. 12 — Microthermal probe response at forward hanger bay door location from (a) 1453 and (b) 1511 hours on 24 March

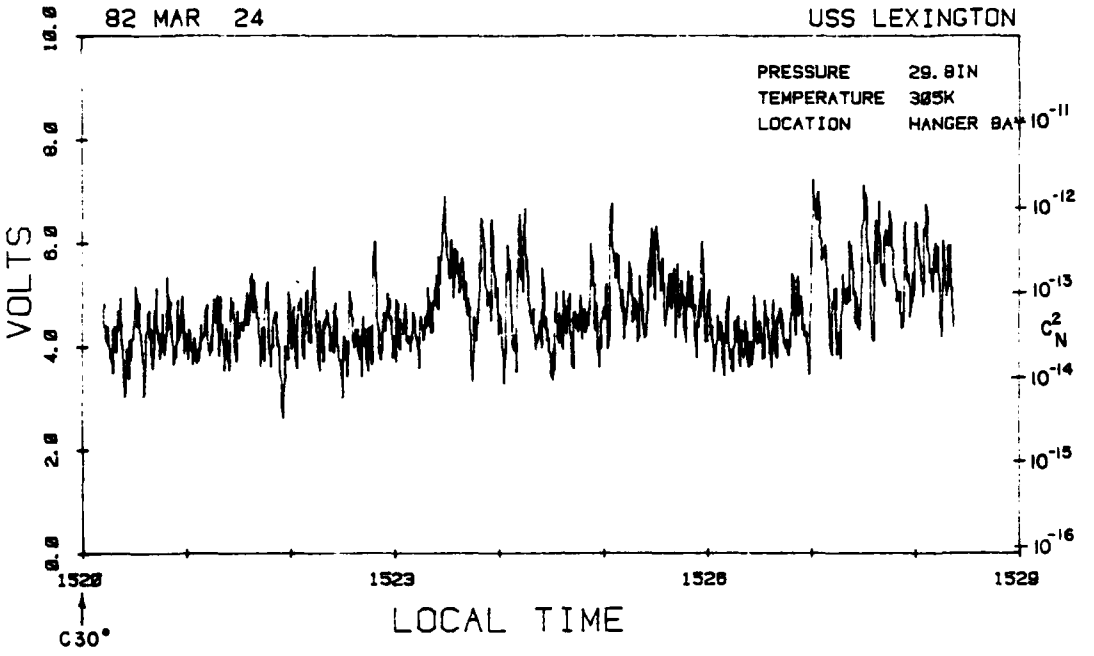

(c)

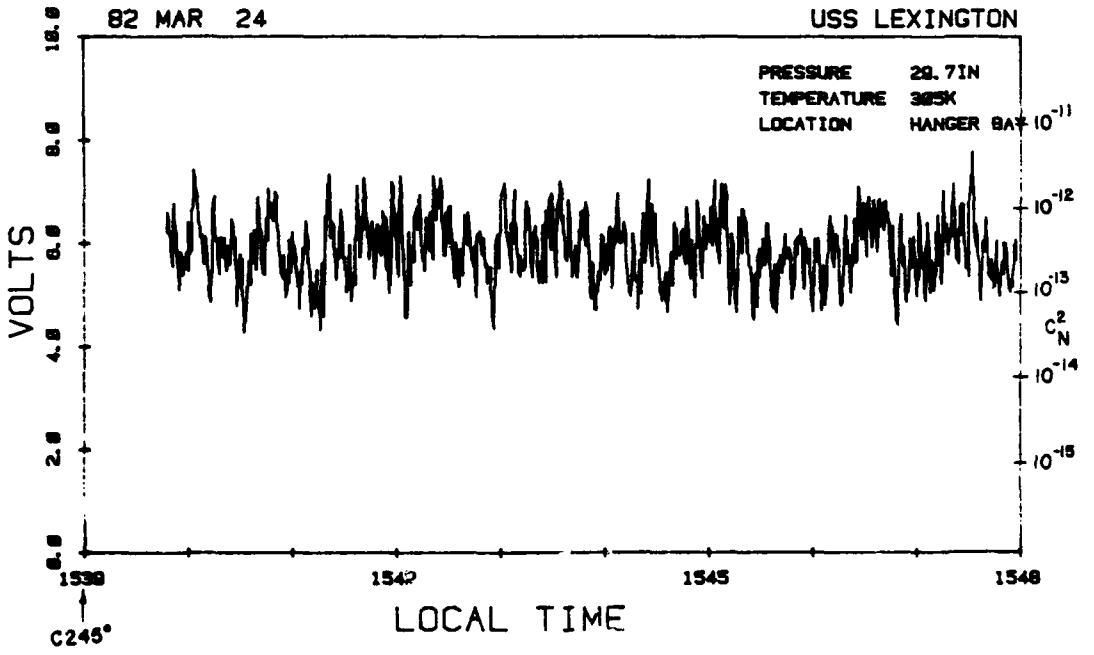

(d)

Fig. 12 — Microthermal probe response at forward hanger bay door location from (c) 1520 and (d) 1530 hours on 24 March

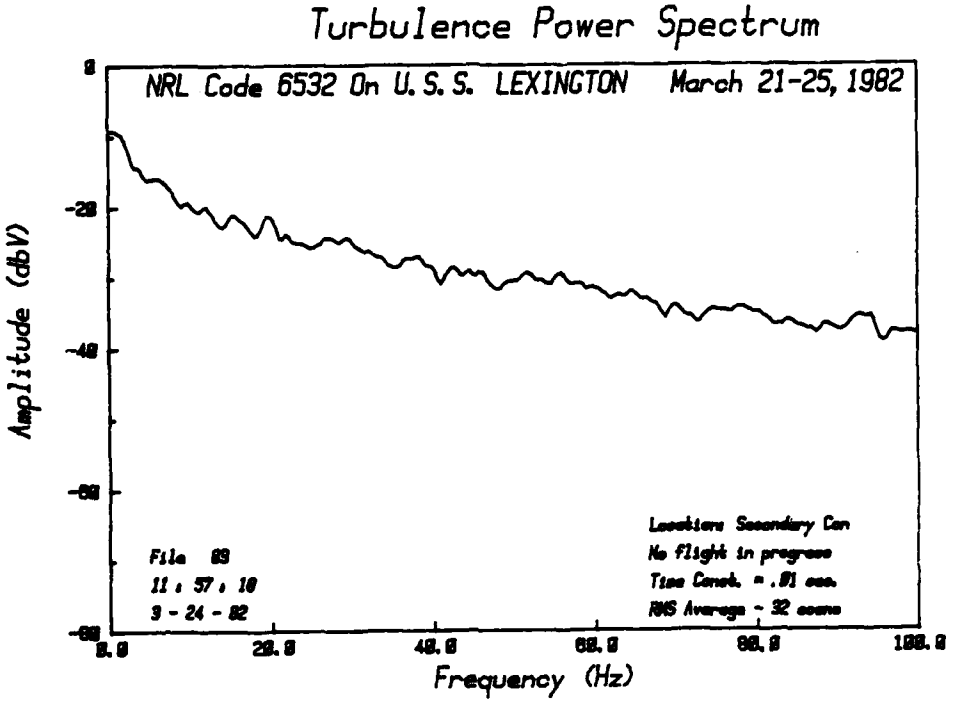

(a)

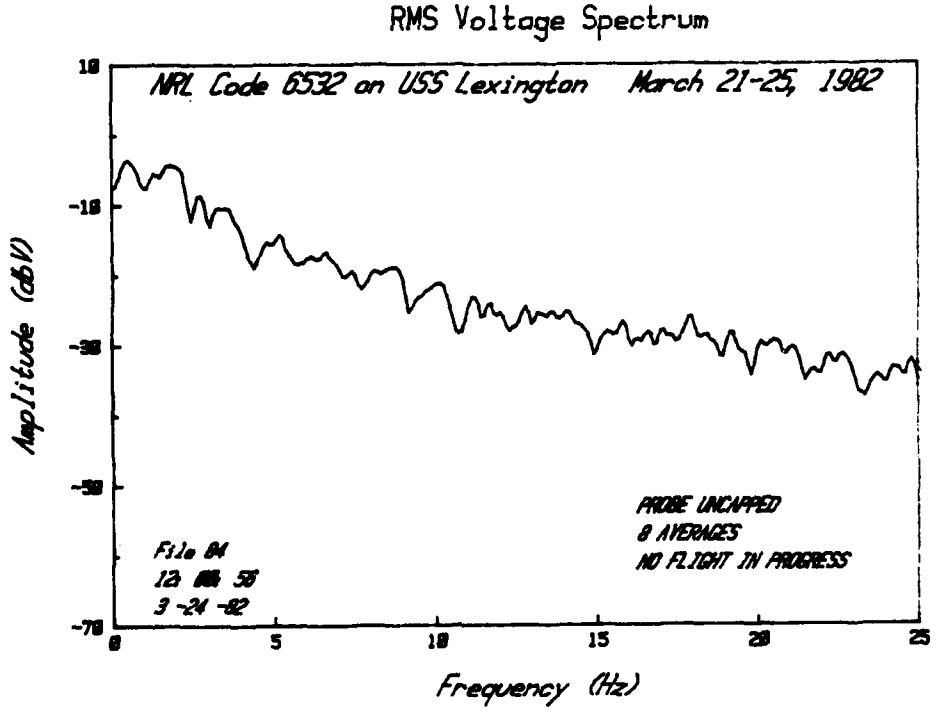

(b)

Fig. 13 – Microthermal probe frequency response measured from (a) 0 to 100 Hz and (b) 0 to 25 Hz

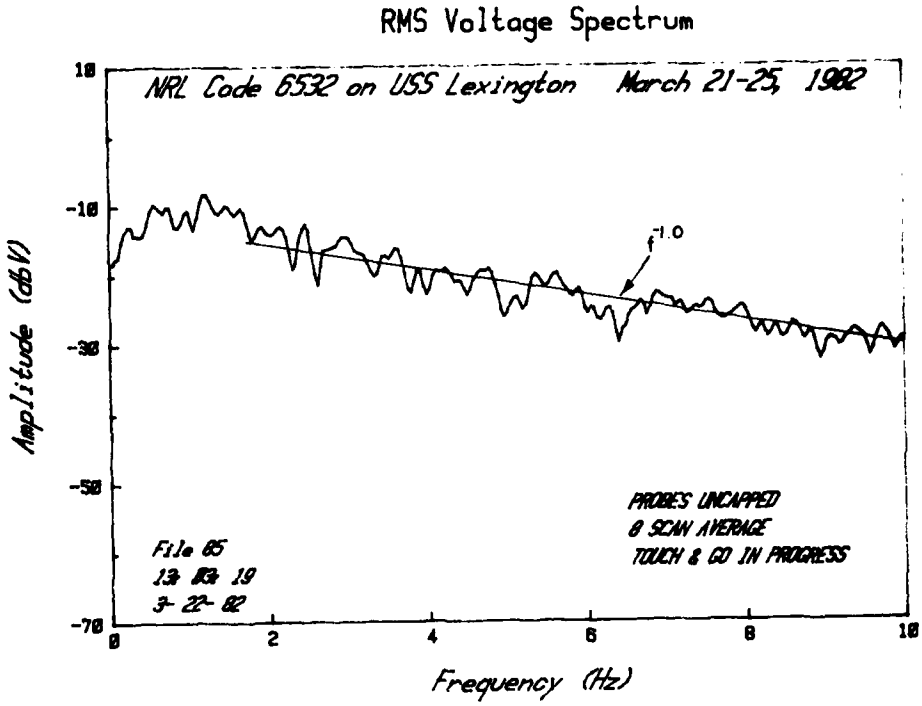

(c)

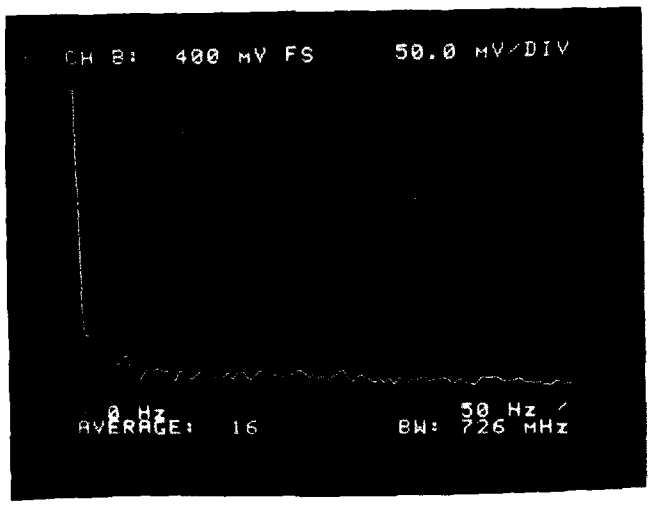

(d)

Fig. 13 – Microthermal probe frequency response measured from (c) 0 to 10 Hz and (d) 0 to 50 Hz with wires capped

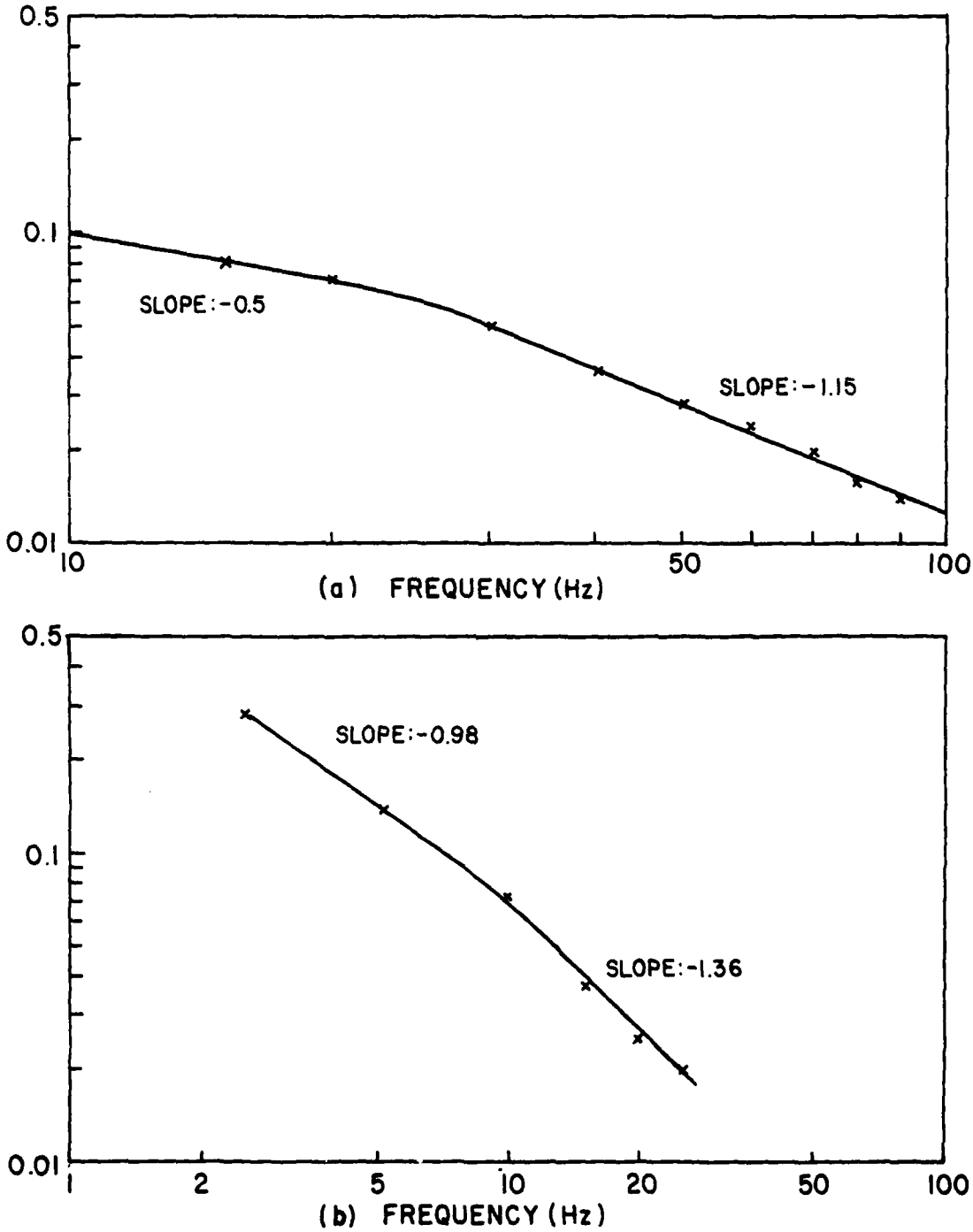

Fig. 14 – Best fit RMS microthermal fluctuation curves plotted on log-log scale

References

1. R. F. Horton, "Preliminary Shipboard Optical Turbulence Measurements," Atmospheric Effects on Electro-Optical, Infrared and Millimeter Wave Systems Performance Conference, San Diego (27, 28 August 1981) SPIE Proceedings Volume 305.
2. C. A. Friehe, "Estimation of the Refractive-Index Temperature Structure Parameter Over the Ocean," Applied Optics, Volume 16, p 334, 1977.
3. G. L. Trusty, T. H. Cosden, S. Craig, and P. C. Ashdown, "Measurements of Optical Propagation Parameters Aboard the Aircraft Carrier USS LEXINGTON," NRL Memorandum Report 4716 (December 31, 1981).
4. Microthermal Probe System - Model MT2 Manual and supplementary notes, Contel Inc., Oregon.
5. R. W. Harris, "Optimization of Probe Excitation for a Two-Probe Measurement of the Refractive-Index Structure Function Constant of the Atmosphere", NRL Report 7587 (July 31, 1973)
6. P. Lebow, "Guide for Computer Controlled Operation of HP3582A Spectrum Analyser Using a HP85 Desk Top Calculator," NRL Memorandum (in preparation).
7. C. W. Fairall, K. L. Davidson and G. E. Schacher, "Humidity Effects and Sea Salt Contamination of Atmospheric Temperature Sensors," Journal of Applied Meteorology, Volume 18, p. 1237, 1979.
8. C. W. Fairall, G. E. Schacher and K. L. Davidson, "Measurements of the Humidity Structure Function Parameters, C_q^2 and C_{TQ}, over the Ocean," Boundary-Layer Meteorology, Volume 19, p 81, 1980.
9. K. L. Davidson, G. E. Schacher, C. W. Fairall and A. K. Goroch, "Verification of the Bulk Method for Calculating Overwater Optical Turbulence," Applied Optics, Volume 20, p 2919, 1981.

10. D. H. Leslie, P. B. Ulrich and G. L. Trusty, "Technical Analysis of a Proposed Ship-to-Ship Chemical Laser Transmission Experiment," NRL Memorandum Report 4745 (February 16, 1982).

11. W. L. Wolfe and G. J. Zissis, Editors, "The Infrared Handbook," Office of Naval Research, Washington, D.C., 1978, Chapter 6.

12. J. R. Kerr, "Experiments on Turbulence Characteristics and Multiwavelength Scintillation Phenomena," JOSA, Volume 62, p 1040, 1972.